Human CTF18-RFC complexed with DNA polymerase ε loads PCNA efficiently and maintains the DNA synthesis

藤澤, 遼

https://doi.org/10.15017/1931744

出版情報：九州大学, 2017, 博士（理学）, 課程博士
バージョン：
権利関係：

Human CTF18-RFC complexed with DNA polymerase ε loads PCNA efficiently and maintains the DNA synthesis

ヒト DNA ポリメラーゼ ε と結合した CTF18-RFC による PCNA ローディングはその DNA 合成の継続に寄与する

九州大学大学院 システム生命科学府

分子生命科学 染色体機能学講座

(釣本 敏樹 教授)

平成 25 年度入学

藤澤 遼

平成 30 年 1 月 22 日提出

CONTENTS

Abbreviations

APB: 4-azidophenacyl bromide, ATP: adenosine triphosphate, ATPγS: adenosine-5′-O-(3-thiotriphosphate), ATR: Ataxia telangiectasia and Rad3 related protein, BSA: bovine serum albumine, CBB: coomasie brilliant blue, Cdc: Cell division cycle, CDK, Cell cycle-dependent kinase, Cdt1: Cdc10-dependent transcript 1, CHAPS: 3-[(3-cholamidopropyl) dimethyl ammonio] propane sulfonate, CMG: Cdc45-Mcm2–7-GINS, CTF: Chromosome Transmission Fidelity, CV: column volume, DCC1: Defective in sister Chromatid Cohesion 1, DDK, *Dbf4*-Dependent Kinase, dpb: DNA Polymerase B subunit, DEAE: diethylaminoethyl, dsDNA: double strand DNA, DTT: dithiothreitol, EDTA: ethylenediamine tetra acetic acid, Elg: Enhanced Level of Genomic instability, EMSA: electrophoretic mobility shift assay, exo–: exonuclease deficient, FenI: Flap end nuclease I, GINS: Go-ichi-ni-san, HBS: Hepes Buffered Saline, Hepes: 4-(2-hydroxyethyl)-1-piperazineethanesulfonic acid, HU: hydroxyl urea, Mcm: Mini chromosomal maintenance, Mrc1: Mediator of the replication checkpoint 1, NP-40: Nonidet P-40, nt: nucleotide, ORC: Origin recognition complex, PBS: Phosphate buffered saline, PCNA: Proliferating cell nuclear antigen, PMSF: phenylmethylsulfonyl fluoride, Pol: DNA polymerase, pre-RC: pre-replicative complex, Psf1: Partner of sld five, Rad: Radiation sensitive, PVDF: polyvinylidene difluoride, RFC: Replication factor C, RPA: Replication protein A, SDS: sodium dodecyl sulfate, SDS-PAGE: sodium dodecyl sulfate-polyacrylamide gel electrophoresis, sld: synthetic lethal with *dpb11-1*, ss: single strand, Tris: tris hydroxymethyl aminomethane, WT: wild type, 3′ primer-template junction: 3′-end recessed primer-template junction

ABSTRACT

At initiation of DNA replication in eukaryotic cells, “replisome”, a high-ordered protein assembly is formed to unwind double-stranded DNA and synthesize leading and lagging strands coordinately. The replicative DNA helicase complex, CDC45-MCM2–7-GINS (CMG) complex recruits three distinct DNA polymerases (Pol) α, δ, and ε, which are specialized to synthesize RNA/DNA hybrid primers, lagging- and leading-strand DNAs, respectively. A toroidal protein complex, proliferating cell nuclear antigen (PCNA) functions as a DNA sliding clamp, which encircles double-stranded DNA to provide an assembly platform for various replisome proteins including Pols.

Polε is required for the leading-strand synthesis, specifically forming a stable complex with an alternative PCNA loader complex CTF18-RFC via the N-terminal half of the catalytic p261 subunit (p261N). Unlike the canonical PCNA loader RFC, CTF18-RFC alone has a limited clamp-loading activity under physiological conditions. I found that CTF18-RFC complexed with Polε restored the activity and became an alternative of RFC. This suggests that CTF18-RFC functionally loads PCNA especially when it forms complex with Polε. A 3′-end recessed primer-template junction is the target DNA structure for efficient PCNA loading of the CTF18-RFC–Polε complex. Proteins directly interacting with the primer-template junction DNA were analyzed in the presence of CTF18-RFC, PCNA, and p261N by site-specific photo-crosslinking. p261N bound to the target site most of the time and binding of CTF18-RFC was limited. However, in the presence of ATPγS, the binding of CTF18 increased. Thus, CTF18-RFC complexed with Polε would access to the primer terminus for PCNA loading transiently. Polε could be placed in DNA synthesis mode using a deoxidized 3′ primer end. I demonstrated that CTF18-RFC complexed with synthesizing mode of Polε exhibited less efficient PCNA loading, indicating that DNA synthesis and PCNA loading of the CTF18-RFC–Polε complex are mutually exclusive at the 3′-end of a primer-template junction. In a DNA synthesis mode, PCNA and the CTF18-RFC–Polε complex engaged in stable trimeric assembly on the template DNA and actively synthesized DNA. Therefore, the CTF18-RFC–Polε complex will be an active configuration of the leading-strand DNA polymerase, in which CTF18-RFC will monitor and, if necessary, restore DNA synthesis by *de novo* loading of PCNA.

In summary, two sets of PCNA loader and DNA polymerase in eukaryotes have distinct roles for leading- and lagging-strand DNA synthesis. RFC and Polδ respectively target free 3′ primer ends and will be most applicable for discontinuous lagging-strand synthesis, whereas,

CTF18-RFC and Polε form a stable complex along with the loaded PCNA at synthesizing 3′ DNA ends and will be specialized to maintain continuous leading-strand synthesis.

Introduction

Eukaryotic DNA replication

DNA replication is a fundamental process for all living organisms. Its dysregulation leads to spontaneous mutations, DNA damage and gross chromosomal rearrangements. These genomic instabilitys cause cell senescence and cancer cell development (Weinert et al., 2009, Truong and Wu, 2011, Lopez et al., 2014, Gaillard et al., 2015, Tomasetti and Vogelstein, 2015). Unlike prokaryotes' genomes, eukaryotes' genomes have multiple replication origins (Leonard and Méchali, 2013). To maintain the gene dosage constant through cell divisions, the activation of replication origins must occur only once per cell-cycle, and strict regulation for the loading and activation of replicative helicase ensures the mechanism (Bell and Labib, 2016). Recent studies with purified proteins of *S. cerevisiae* have demonstrated the reconstitution of origin dependent DNA replication (Yeeles et al., 2015, 2017, Devbhandari et al., 2016, Lõoke et al., 2017).

The mechanism of replication initiation in *S. cerevisiae* will be described as follows; The six subunits complex ORC (Origin Recognition Complex) binds to the replication origin in the presence of ATP (Bell and Stillman, 1992, Diffley and Cocker, 1992, Li and Stillman, 2012). Using the ORC as the assembly platform, pre-RC (pre-replication complex) is formed with two Mcm2–7 complexes, the hexametric AAA+ motor core of the replicative helicase in collaboration with Cdc6 and Cdt1 from telophase to G1 phase when CDK/cyclin levels are low (Evrin et al., 2009, Remus et al., 2009, Riera et al., 2014). In S phase when the activities of two essential kinases, DDK and S-CDK increase, sequential protein recruitments including Sld3-Sld7-Cdc45, Dpb11, Sld2, GINS, Mcm10, and Polε occur on the phosphorylated Mcm2–7 in a head to head configuration, resulting in formation of the active replicative DNA helicase CMG consisted of Cdc45, Mcm2–7 and GINS (Kamimura et al., 2001, Tanaka et al., 2007, Zegerman and Diffley, 2007, Muramatsu et al., 2010, Yardimci et al., 2010, Heller et al., 2011, Deegan et al., 2015, Riera et al., 2017). Upon completion of the assembly, two CMG helicases bidirectionaly translocate on the leading-strand template DNA in a 3′-5′ direction to unwind duplex DNA (Fu et al., 2011, Yu et al., 2014).

Eukaryotic DNA polymerases and the elongation process

To date 16 DNA-dependent DNA polymerases are identified in human cell (Vaisman and Woodgate, 2017). Among them, Polα, Polδ, and Polε are replicative DNA polymerases for genomic DNA replication in nucleus, unlike that only one replicative DNA polymerase III is responsible for replication of eubacteria genome (Mclnerney et al., 2007, Johansson and Dixon,

2013). Polα, Polδ, and Polε are composed of one catalytic subunit and other two or three subunits and in division of labour in the replisome. The CMG helicase associates with Polε via the interaction between Dpb2/p59 second subunit of Polε and Psf1 subunit of GINS (Sengupta et al., 2013) and synthesizes leading-strand DNA processively (Pursell et al., 2007, Georgescu et al., 2014, Daigaku et al., 2015). The other replicative DNA polymerase Polα complexed with the primase is also connected physically with CMG helicase via Ctf4, which functions as a hub in replisome (Gambus et al., 2009, Tanaka et al., 2009, Villa et al., 2016). Polα synthesizes short RNA/DNA primer on unwound ssDNA of the lagging-strand DNA template (Pellegrini, 2012, Georgescu et al., 2015a). The third DNA polymerase Polδ synthesizes lagging-strand DNA discontinuously (Nick McHelinny et al., 2008, Daigaku et al., 2015) without direct connection with CMG helicase (Sun et al., 2015, Schauer and O'Donnell, 2017). The discontinuous lagging-strand DNAs are processed by FenI and Dna2 nucleases and ligated by Lig1 (Bae et al., 2001, Stith et al., 2008). Since most of yeast replication proteins are conserved in metazoan (Bell and Labib, 2016), the basic principles of DNA replication among eukaryotes are suggested to be identical.

Polδ and Polε possess a 3′-5′ exonuclease activity and highly accurate fidelity for DNA polymerization activity (Kunkel et al., 1987, Morrison et al., 1990, 1991). For efficient, processive DNA synthesis, however, they require additional factors (Masuda et al., 2007, Chilkova et al., 2007) such as RPA (Replication Protein A), PCNA (Proliferating Cell Nuclear Antigen), and RFC (Replication Factor C). RPA is a single-stranded DNA binding protein, resolving secondary structure of ssDNA (Fanning et al., 2006). PCNA is a ring-shaped sliding clamp protein, clamping DNA polymerase onto DNA for their stable DNA synthesis, and its loader, RFC loads PCNA at a 3′-end recessed primer-template junction (3′ primer-template junction) DNA with ATP-hydrolysis actions (see below sections). Thus, these factors are also essential components of the replisome. PCNA forms a homo-trimeric ring complex embracing double-strand DNA in its central hole (Krishna et al., 1995), and slides along DNA freely at 100-150 bp/0.2 microseconds (De March et al., 2017). This sliding clamp interacts not only with replicative DNA polymerases, but also with various proteins involved in translesion DNA synthesis, Okazaki fragment processing, chromatin assembly, DNA methylation, DNA damage response and sister chromatid cohesion (Moldovan et al., 2007, Choe and Moldovan, 2017). Thus, PCNA provides a reaction-platform on replicating DNA not only for DNA synthesis but also for diverse range of reactions (Bell and Labib, 2016).

The replicative leading-strand DNA polymerase, Polε

Polε consists of four subunits, Pol2, Dpb2, Dpb3, and Dpb4 in *S. cerevisiae* (Chilkova et al., 2003), and p261/POLE1, p59/POLE2, p17/POLE3, p12/POLE4 in *H. sapiens* (Li et al., 1997). Pol2 (p261 in human) encoding the catalytic subunit and Dpb2 (p59 in human) are essential, whereas Dpb3 and Dpb4 (p17 and p12 in human) are non-essential in yeast (Araki et al., 1991a, Araki et al., 1991b, Ohya et al., 2000). A unique property of Polε is that its catalytic subunit consists of two tandem exonuclease-polymerase modules, but N-terminal one is only catalytically functional (Tahirov et al., 2009). In *S. cerevisiae* and *S. pombe*, its N-terminal polymerase domain is dispensable, while the inactive C-terminal one is necessary for cell viability (Kesti et al., 1999, Feng and D'Urso, 2001). Thus, the essential Polδ will complement Polε to synthesize leading-strand DNA when its catalytic activity is nonfunctional (Miyabe et al., 2015, Yeeles et al., 2017). The C-terminal module along with Dpb2 plays a role for assembly of CMG helicase by recruiting GINS complex to pre-RC, and keeps the coupling with CMG helicase during replisome progression (Muramatsu et al., 2010, Handa et al., 2012, Kang et al., 2012, Yeeles et al., 2015, 2017). Dpb3 and Dpb4 form a hetero-dimer via their histone-fold like structures, bind to dsDNA (Tsubota et al., 2006), and are important for the processivity of both DNA synthesis and exonucleolytic degradation (Aksenova et al., 2010).

In addition to its direct roles in DNA replication, Polε has diverse roles, such as in DNA repair (Moser et al., 2007, Ogi et al., 2010), epigenetic information inheritance (Iida and Araki, 2002, Tsubota et al., 2006, Li et al., 2011), cell senescence (Deshpande et al., 2011, Saka et al., 2016) and S-phase checkpoint response (Navas et al., 1995, 1996, Dmowski et al., 2017). The replisome inevitably encounters stochastic disassembly or stalling by various obstacles as DNA damage on template DNA and by deficiency of dNTP. Under such circumstances, checkpoint kinases Mec1-Rad53 in *S. cerevisiae*, and ATR-Chk1 in vertebrate are activated and regulate the ribonucleotide reductase activity, the temporal program of replication origin firing, and cell cycle progression. (Giannattasio and Branzei, 2017, Saldivar et al., 2017). Because Polε is the primary DNA polymerase for leading-strand DNA, Polε might monitor its own DNA synthesis state in leading-strand DNA and transduce signals to checkpoint pathway (Puddu et al., 2011). Indeed, mutations in the C-terminus of Pol2 affect the S-phase checkpoint function (Navas et al., 1995), and the presence of the catalytically functional Polε in replisome is required to activate Rad53 (García-Rodríguez et al., 2015). Polε also interacts with the checkpoint mediator protein Mrc1/CLASPIN, and one of the alternative PCNA loader Ctf18-RFC as described below, both of which are implicated in the checkpoint response (Lou et al., 2008, García-Rodríguez et al., 2015).

Even with tight relevance between replisome and the checkpoint response, the actual mechanism in checkpoint response mediated thorough Polε is still poorly understood.

The alternative PCNA loader, CTF18-RFC

Clamps and their loader complexes are the essential components for DNA replication in all organisms. Loader complexes consist of five similar or same AAA+ ATPase family proteins. As exemplified above, the eukaryotic canonical loader for PCNA clamp is RFC, consisting of one large subunit (RFC1) and four small subunits (RFC2–5) (Bloom, 2009, Hedglin et al., 2013, Kelch, 2016). An ATP-bound form of RFC binds to PCNA (Shiomi et al., 2000, Gomes and Burgers, 2001), opens PCNA ring structure and further binds to the 3′ primer-template junction (Tsurimoto and Stillman, 1991, Hingorani and Coman, 2002, Shiomi et al., 2004). Upon binding, RFC hydrolyses ATP and leaves from PCNA and DNA (Sakato et al., 2012, Marzahn et al., 2015), consequently the loaded PCNA staying on DNA.

Three RFC1 paralogues, Ctf18, Rad17 (Rad24 in *S. cerevisiae*) and Elg1, exist in eukaryotes and associate with RFC2–5 to form alternative clamp loader complexes, Ctf18-RFC, Rad17-RFC and Elg1-RFC. Ctf18-RFC and Elg1-RFC target PCNA (Berumudez et al., 2003, Kanellis et al., 2003), whereas the checkpoint loader Rad17-RFC targets the checkpoint clamp Rad9–Hus1–Rad1 (9-1-1 complex; Ddc1–Rad17–Mec3 in *S. cerevisiae*; Ellison and Stillman, 2003, Navadgi-Patil and Burgers, 2009) for the activation of checkpoint kinases (Saldivar et al., 2017). Elg1-RFC functions as a PCNA unloader (Kubota et al., 2013a, Shiomi and Nishitani, 2013, Yu et al., 2014). As compared to other clamp loader complexes, actual functions of Ctf18-RFC as a clamp loader are less understood.

Ctf18-RFC has two additional subunits, Dcc1 and Ctf8, and forms a heptameric-subunit complex (Mayer et al., 2001, Merkle et al., 2003). *CTF18, DCC1,* and *CTF8* were originally identified as genes whose defects resulted in mitotic chromosome stability (Spencer et al., 1990, Kouprina et al., 1993). Ctf18, Dcc1 and Ctf8 function together, and are involved in the same epistasis group. Their defects affect a variety of DNA replication-coupled events such as double strand break-recombination repair, chromatin regeneration, triplet repeats stability and proper telomere maintenance (Hiraga et al., 2006, Ogiwara et al., 2007, Khair et al., 2010, Gellon et al., 2011, Foltman et al., 2013, Gao et al., 2014). Important feature of Ctf18-RFC is its requirement for sister chromatid cohesion, which ensures faithful segregation of replicated sister chromatids (Mayer et al., 2001, Hanna et al., 2001, Xu et al., 2007, Takahashi et al., 2010). This explains why mutations of *CTF18* affect mitotic chromosome stability. The ring-shaped SMC complex,

cohesin entraps replicated sister chromosomes until anaphase (Michaelis et al., 1997, Losada et al., 1998, Peters and Nishiyama, 2012, Uhlmann, 2016). One of the key steps in the establishment of sister chromatid cohesion is acetylation of Smc3 cohesin subunit mediated by cohesin acetyltransferase Eco1 (xEco1/xEco2 in Xenopus and Esco1/Esco2 in human; Skibbens et al., 1999, Hou and Zou, 2005, Zhang et al., 2008), leading the cohesin to be resistant to its unloading factors Wapl-Pds5 (Rolef Ben-Shahar et al., 2008, Sutani et al., 2009). Eco1 interacts with PCNA for its efficient acetylation of Smc3 (Moldovan et al., 2006, Higashi et al., 2012, Song et al., 2012). Ctf18-RFC is suggested to contribute for the proper function of cohesin acetyltransferase at the replication fork via its loading of PCNA (Lengronne et al., 2006, Terret et al., 2009, Borges et al., 2013). Ctf18-RFC also functions in S-phase checkpoint response redundantly with the Ddc1–Rad17–Mec3 complex and Rad24-RFC in *S. cerevisiae* (Naiki et al., 2001, Ansbach et al., 2008, Crabbé et al., 2010, Kubota et al., 2011, García-Rodríguez et al., 2015). Its deficiency partially reduces the activation of Rad53/Cds1 checkpoint kinase, and leads to the firing of dormant replication origins under replication stress condition.

Ctf18 localizes at the replication fork and recruits a subpopulation of PCNA in *S. cerevisiae* (Lengronne et al., 2006, Kubota et al., 2011). In metazoan, such as worm, xenopus, and human, Ctf18 (CTF18) is also enriched at the replication fork (Sirbu et al., 2013, Alabert et al., 2014, Dewar et al., 2017, Sonneville et al., 2017). In human cell, CTF18-RFC contributes for PCNA-dependent Cdt1 degradation during S-phase, differentially from RFC (Shiomi et al., 2012). Knockout of DCC1 in human cell severely affects cell proliferation, and the cells showed hypersensitivity to HU and aphidicolin, leading to cell senescence, indicating that the functional CTF18-RFC complex might be required for normal replication-fork progression, DNA-damage response and proper cohesion establishment (Terret et al., 2009). Knockout mice of CTF18 (CHTF18) are viable, although they show slow embryonic development, and have a defect in meiotic recombination (Berkowitz et al., 2012).

In contrast to these genetic and cell-biological studies, there are less biochemical studies on CTF18-RFC. CTF18-RFC loads PCNA at the 3′ primer-template junction with ATP hydrolysis and supports DNA synthesis by Polδ (Bermudez et al., 2003, Shiomi et al., 2004). It has been reported that in the presence of RPA, Ctf18-RFC directed unloading PCNA (Bylund and Bergers, 2005), though a contradictory result exists that the unloading would not be a major role of Ctf18-RFC *in vivo* (Kubota et al., 2011). One of Y-family DNA polymerases, human Polη is identified as a DNA polymerase that is specifically stimulated by CTF18-RFC (Shiomi et al.,

2007). However, these *in vitro* studies also reported that the presence of DCC1 and CTF8 subunits did not affect significantly in their assay being unable to explain significances of Dcc1 and Ctf8 *in vivo*. Thus, the actual functions of CTF18-RFC in replication fork and variety of events remain to be elucidated.

Ctf18, Dcc1, and Ctf8 function together in the direct interaction of CTF18-RFC with the leading-strand DNA polymerase Polε (Murakami et al., 2010, García-Rodríguez et al., 2015, Okimoto et al., 2016). Their interaction was reported with buddying yeast and human proteins, suggesting that the interaction mechanism is highly conserved. The interaction occurs between the trimeric assembly consisting of CTF18, DCC1, CTF8 and the N-terminal region of the catalytic subunit Pol2/p261 of Polε (Murakami et al., 2010, García-Rodríguez et al., 2015). In *S. cerevisiae*, the interaction in DNA replication fork is required for activation of the Mec1-Rad53-dependent checkpoint pathway (García-Rodríguez et al., 2015) and maintenance of genome stability (Okimoto et al., 2016). Because either defect of ctf18, dcc1 or ctf8 leads to loss of the interaction with Polε and also diverse defects in cellular activities, understanding of the biochemical significance of their interaction is necessary.

In this study, I demonstrated functional significances of their interaction by variety of biochemical analyses. Though CTF18-RFC alone has a limited PCNA loading activity in near-physiological conditions, it restores the activity when it forms a complex with Polε and can load PCNA at a 3′ primer-template junction. Furthermore, I examined how the complex binds to 3′ primer-template junctions during PCNA loading. Polε occupies the target structure most of the time, but CTF18-RFC transiently accesses it for PCNA loading. CTF18-RFC loads PCNA efficiently when Polε is not in DNA synthesizing mode. In addition to the efficient PCNA loading, Polε, CTF18-RFC and the loaded PCNA form a stable complex at the 3′ primer end and synthesize DNA more efficiently than Polε with PCNA loaded by RFC. These results indicate that CTF18-RFC will be involved in the replisome through interaction with Polε and load PCNA by monitoring the DNA synthesis mode of Polε to maintain efficient synthesis of the leading-strand DNA.

MATERIALS AND METHODS

Buffers

PBS: 140 mM NaCl, 2.8 mM KCl, 6.1 mM Na_2HPO_4, and 1.7 mM NaH_2PO_4. (TaKaRa)

Buffer H: 25 mM Hepes [4-(2-hydroxyethyl)-1-piperazineethanesulfonic acid]-NaOH (pH7.8), 1 mM EDTA (ethylenediamine-tetra-acetic acid), 0.01% (v/v) NP-40 (Nonidet P-40) and 10% (v/v) glycerol.

Buffer B: 50 mM Tris [tris(hydroxymethyl)aminomethane]-HCl (pH8.0), 1 mM EDTA and 10% (v/v) glycerol.

PC Buffer: 50 mM KPO_4 (pH7.5), 1 mM EDTA, 1 mM CHAPS (3-[(3-Cholamidopropyl) dimethyl ammonio] propane sulfonate), 10% (v/v) glycerol

Buffer AK: 0.01% (v/v) NP40, 10% (v/v) glycerol and indicated concentration of KPO_4 (pH7.5)

1×HBS: 10 mM Hepes-NaOH (pH7.8), 3.2 mM EDTA, 0.05% (v/v) Tween20 and 0.15 M NaCl

loading buffer: 10 mM Hepes-NaOH (pH7.8), 0.05% (v/v) Tween20, 10 mM $MgCl_2$, 0.2 mM EDTA, 0.01% (w/v) BSA and 0.5 mM DTT

2×SDS sample buffer: 100 mM Tris-HCl (pH6.8), 200 mM DTT, 4% (w/v) SDS, 0.1% (w/v) bromophenol blue and 20% (v/v) glycerol.

Running buffer for SDS-PAGE (polyacrylamide gel electrophoresis): 25 mM Tris, 20 mM glycine and 0.1% (w/v) SDS.

Transfer buffer for immunoblotting: 25 mM Tris and 20 mM glycine.

TBS-T: 30 mM Tris-HCl (pH7.5), 200 mM NaCl and 0.1% (v/v) Tween20.

TE: 10 mM Tris-HCl (pH8.0) and 1 mM EDTA

BW Buffer: 1 M NaCl, 10 mM Tris-HCl (pH8.0)

SDS-PAGE and Immunoblotting

Protein samples were mixed with SDS sample buffer, heated at 95˚C for 3 min, and applied to SDS-PAGE in 10, 12.5 or 15% (w/v) polyacrylamide gel. Proteins in polyacrylamide were transferred to Hybond-P PVDF membrane (GE Healthcare) with semi-dry blotting apparatus with transfer buffer at 1.5 mA/cm^2 for 1 h. The membrane was masked with 2.5% (w/v) skim milk in TBS-T (TBS-T milk) for 30 min, washed for 5 min with TBS-T 3 times, and incubated with the primary antibody in TBS-T milk or CANGETSIGNAL solution1 (TOYOBO) at RT for 1 h. Subsequently, the membrane was washed for 5 min 3 times with TBS-T, incubated with the secondary antibody in TBS-T milk or CANGETSIGNAL solution2 (TOYOBO) at RT for 1 h and soaked in ECL Detection Reagent (GE Healthcare) after 3 washes with TBS-T for 5 min. The

reacted protein bands were visualized with LAS-3000mini (FUJIFILM). For CBB staining of separated proteins in the gels, Rapid stain CBB Kit (nacalai tesque) was used.

Antibodies

Anti-CTF18 mouse monoclonal antibody (ABNOVA M01 886-975: 1/2000), a culture sup of the mouse hybridoma producing anti-Polε p261 monoclonal antibody (ATCC CRL-2284: 1/1), anti-Polδ p125 goat polyclonal antibody (Santa Cruz C-20, sc-8769: 1/3000), anti-PCNA rabbit polyclonal antiserum (Laboratory preparation C-2: 1/3000), anti-RPA polyclonal antibody (Laboratory preparation: 1/2000), anti-mouse IgG goat antibody conjugated with HRP (Bio-Rad, 170-6516: 1/2,000), anti-rabbit IgG goat antibody conjugated with HRP (Bio-Rad, 170-6515: 1/2,000), were used at indicated dilution rates.

Construction of the baculovirus for expression of His-p261N^{exo-}

A recombinant baculovirus (bv) to express His-p261N^{exo-}, a mutant of human p261N, which harbors from 1 to 1342 residues of p261 with the substitution of D275, the highly conserved residue in the exonuclease domain (Henninger and Pursell, 2014) to alanine was prepared as follows: 261Nter cassette containing a stop-codon substitution at the 1342 residue was prepared by annealing of p260NFw and p260EcoRV, and inserted between FseI and EcoRI ends of pBacPAKHisp261^{D275A} (This plasmid has the full-length coding sequence of p261 with the mutation of D275A; a kind gift from Dr. Kouji Hirota, Tokyo Metropolitan University). The resulted plasmid, pBacPAKHisp261N^{D275A}-6 was then treated with SalI. The 4 kb DNA fragment carrying p261N^{D275A} coding sequence was separated and inserted into pFastbac1 vector using its SalI end and blunted XbaI ends, and pFastBac p261N^{D275A}-1 was then modified to pFastBac His p261N^{D275A}-3 by in-frame insertion of HisSalI cassette prepared by annealing of HisSalIFw and HisSalIRv at the *Sal*I site, locating in front of the start codon of p261N^{D275A}. The baculovirus genome DNA for expression of His-p261N^{exo-} was obtained by transposition of the Tn7 unit of the donor plasmid into the bacmid genome in *E.coli* DH10Bac (Invitrogen) by 72 h culturing after transformation. The resulted recombinant bacmid clones appeared as white colonies on an X-gal/IPTG plate were further selected by PCR confirming transposed DNA fragment. The high molecular weight plasmid DNA from a selected colony was prepared and transferred into Sf9 insect cells with Cellfectin (Invitrogen). The culture supernatant was recovered 72 h post-transfection and a genuine virus clone expressing His-p261N^{exo-} was isolated after single-plaque isolation from the supernatant as bvHis-p261N^{exo-}.

Amplification of baculoviruses

1.0×10^7 Sf9 insect cells, which is cultured at 0.5-2.0×10^6 cells/ml in a spinner flask, were plated onto a 150 mm culture dish with 20 ml of Grace medium (GIBCO) supplemented with 10% (v/v) FBS (Fetal Bovine Serum), 100 units/ml penicillin, and 100 μg/ml streptomycin. After adhesion of the cells to a dish, the medium was removed and an appropriate volume (typically 0.1-0.5 ml) of culture sup containing bv for expression of an aimed protein was added to the dish by mixing with the same medium up to 3 ml, and left at RT for infection. After 1 h, the same medium was added up to 20 ml and the cells were incubated at 27˚C for 72 h. The culture sup was collected by centrifugation at 800 g for 5 min and stored at 4˚C.

Expression of recombinant proteins with baculoviruses

bv for expression of human proteins were amplified from laboratory stocks (Shiomi et al., 2007, Narita et al., 2010, Murakami et al., 2010) or newly prepared as bvHis-p261N^{exo-}. All epitope-tags were inserted at the N-termini of target proteins. 1.5×10^7 High5 insect cells, maintained at 0.5-2.0×10^6 cells/ml in a spinner flask, were plated onto a 150 mm culture dish with Express five medium (GIBCO) supplemented with L-glutamine, 100 units/ml penicillin, and 100 μg/ml streptomycin. After adhesion of the cells to dish, medium was removed and Sf9-culture sups containing bv were added to the dish by mixing the same medium up to ~4 ml. RFC and Polδ complexes were expressed by mixed infections of bvFLAG-RFC1, bvp40, bvp38, bvp37 and bvp36 or of bvp125, bvp66, bvHis-p50, and bvp12 in ratios optimized by pilot experiment. CTF18-RFC or CTF18-RFC(5) complexes were prepared by mixed infections of byFLAG-CTF18, bvp40, bvp38, bvp37 and bvp36 with or without bvDCC1 and bvCTF8. Polε and Polε^{exo-} were prepared with bvHis-p261 or bvHis-p261^{exo-} along with bvFLAG-p59, bvp17 and bvp12. p261N and p261N^{exo-} proteins were prepared by infection of bvHis-p261N^{WT} and bvHis-p261N^{exo-} respectively. After 1 h infection at RT, fresh Express five medium was added up to 20 ml and the cells were incubated at 27˚C for 48 h, except for CTF18-RFC and CTF18-RFC(5) for 72 h. After expression, cells in 150 mm dishes were washed with 5 ml PBS, and suspended with 0.8 ml of Buffer B per dishes containing 0.15 M NaCl, 2 μg/ml leupeptin (Peptide Institute) and 0.1 mM PMSF (nacalai tescue). The cells were lysed by addition with final 0.5% (v/v) NP-40 and vigorous mixing with vortex for 30 sec. The samples was left on ice for 10 min and further added with final 0.5 M NaCl followed by incubation on ice for 20 min and applied to centrifugation at 66,000 g for 30 min at 4˚C. The cell lysate was obtained as the supernatant, frozen with liquid nitrogen and stored at –80˚C.

Purified recombinant human proteins

CBB staining profile after SDS-PAGE of purified proteins used in this study were shown

in Figure 1. Their protein concentrations were quantified with these CBB bands of the largest subunit mostly, by ImageJ using BSA as a standard.

Purification of RFC, CTF18-RFC, CTF18-RFC(5)

All purification procedures were done at 4˚C unless otherwise noted. A cell lysate from 7.5 x 10^7 High5 cells expressing FLAG-tagged RFC, or CTF18-RFC or CTF18-RFC(5) was applied onto a DEAE sepharose column (2 ml, GE Healthcare) in Buffer B with 0.5 M NaCl. The flow-through fractions were pooled and loaded onto an anti-FLAG antibody sepharose column (1 ml, SIGMA) and washed successively with 5 CV (column volume) of PC buffer with 0.5 M NaCl, 5 CV of PC buffer containing 0.5 M NaCl, 10 mM $MgSO_4$, 5 mM ATP at RT and with 5 CV of PC buffer with 0.5 M NaCl. The target proteins was eluted from the column with 250 µl of PC buffer containing 0.5 M NaCl, 100 µg/ml 1xFLAG peptide (SIGMA), 2 µg/ml leupeptin and 0.1 mM PMSF at 16 times each 4 minutes. The peak fraction (200 µl) was applied to a 5 ml 15-35% (v/v) glycerol gradient sedimentation in PC buffer with 0.1 M NaCl and centrifuged at 220,000 g at 4˚C for 14 h with SW50.1 rotor. After dropwise fractionation of the samples from the bottom of the centrifugation tube, their protein-peak fractions were frozen in liquid N_2 and stored at -80 ˚C.

Purification of p261N^{WT} and p261N$^{exo–}$

A cell lysate expressing His-tagged p261N^{WT} or His-tagged p261N$^{exo–}$ was prepared as above. The lysates were passed through a DEAE sepharose column (2 ml) in Buffer B with 0.5 M NaCl and the unbound fractions were loaded onto a Ni-sepharose High Performance column (1 ml, GE Healthcare), and eluted successively with 10 CV each of Buffer H containing 0.5 M NaCl and 20 mM or 50 mM or 100 mM imidazole. The 100 mM imidazole-eluted fractions containing p261N were pooled and loaded onto a Heparin sepharose 6 Fast Flow column (0.5 ml, GE Healthcare) after 2.5-fold dilution with Buffer H without NaCl. The bound proteins were eluted with 10 CV of a 0.2-1.0 M NaCl gradient in Buffer H. DNA polymerase activities in eluted fractions were monitored with dA/dT [poly dA (ave. 250 nt) and oligo dT (11 nt) at 25 : 1 nucleotides ratio; Pharmacia] as a template (see following sections) and the active p261N fractions around 0.5 M NaCl were pooled, concentrated 5 fold with YM-10000 (Millipore), and centrifuged with a 15-35% (v/v) glycerol gradient in Buffer H with 0.1 M NaCl at 220,000 g at 4˚C for 15 h in SW50.1 rotor. The protein-peaks were collected and stored at -80 ˚C as above.

Purification of Polε^{WT} and Polε$^{exo–}$

Cell lysates and the DEAE sepharose unbound fractions for Polε^{WT} or Polε$^{exo–}$ were prepared as above. The obtained samples were loaded onto an anti-FLAG antibody column (1

ml) and washed with 10 CV of Buffer H with 0.5 M NaCl. The bound proteins were eluted with 4 CV of Buffer H with 0.5 M NaCl and 100 μg/ml 1xFLAG peptide. The eluates were then loaded onto a Ni-sepharose High Performance column (0.3 ml), and the bound proteins were eluted by 5 CV of Buffer H containing 100 mM imidazole and 0.5 M NaCl after a wash with 30 CV of Buffer H with 0.5 M NaCl and 20 mM imidazole. The eluate pool with 100 mM imidazole (200 μl) was purified by glycerol gradient sedimentation, and stored as p261N$^{WT/exo-}$, except for the centrifugation for 11 h.

Purification of Polδ

The DEAE sepharose unbound fractions from a lysate for Polδ was prepared as above and loaded onto a Ni-sepharose High Performance column (1 ml) in Buffer H with 20 mM imidazole and 0.5 M NaCl. The bound proteins were eluted by a 50-250 mM imidazole gradient in 10 CV Buffer H with 0.5 M NaCl after a wash of 5 CV of Buffer H with 50 mM imidazole and 0.5 M NaCl. Fractions containing Polδ bands were pooled and loaded onto MonoQ (1 ml, GE Healthcare) after dilution with Buffer H with 0 M NaCl to 0.1 M NaCl condition. The bound proteins were eluted by a 0.1-0.6 M NaCl gradient in 6 CV of Buffer H. Four-subunit Polδ complex was obtained in fractions eluted with 0.3 M NaCl condition. Their pool were diluted with Buffer H with 0 M NaCl to 0.1M NaCl and loaded onto SOURCE15S (0.25 ml, GE Healthcare). The bound proteins were eluted by a 0.1-0.75 M NaCl gradient in 8 CV Buffer H. The peak fractions (200 μl) around 0.28 M NaCl containing the Polδ complex were pooled, further purified by glycerol gradient sedimentation, and stored as p261N$^{WT/exo-}$, except for the centrifugation at 10˚C for 12 h.

Purification of PCNA

9.6 g of the frozen BL21 (DE3) expressing human PCNA from pT7 PCNA plasmid (Fukuda et al., 1995) was thawed and suspended in 20 ml of Buffer H containing 0.15 M NaCl, 2 μg/ml leupeptin and 0.1 mM PMSF. The cells were lysed by sonication and the supernatant was recovered as the lysate by centrifugation at 66,000 g for 30 min. The lysate was loaded onto a DEAE sepharose column (20 ml) with Buffer H with 0.15 M NaCl, followed by a wash with 5 CV Buffer H with 0.15 M NaCl. The bound proteins were eluted with 5 CV Buffer H with 0.4 M NaCl, and loaded onto a Q-sepharose column (10 ml) after dilution with Buffer H with 0 M NaCl to 0.1 M NaCl, and eluted with an 8 CV gradient of 0.1-0.6 M NaCl in Buffer H. Fractions containing PCNA band around 0.4 M NaCl were pooled and loaded onto Superdex200 (1.5 cm x 50 cm, GE Healthcare) in Buffer H with 0.1 M NaCl. Eluted fractions containing PCNA were pooled and

loaded onto MonoQ, and the bound PCNA was eluted with an 8 CV gradient of 0.1 M-0.6 M NaCl in Buffer H. The peak fractions (200 µl) were pooled and further purified by a glycerol gradient sedimentation and stored as $p261N^{WT/exo-}$, except for the centrifugation at 10 ˚C for 20 h.

Purification of RPA

Rosetta2 carrying p11dt RPA plasmid for expression for human RPA (Henricksen et al., 1994) was cultured in 3.2 L of L-Broth at 37˚C for 16 h and suspended in 30 ml of Buffer H containing 0.5 M NaCl 2 µg/ml leupeptin and 0.1 mM PMSF. The lysate was prepared as PCNA, diluted to 0.1 M NaCl with Buffe H without NaCl and loaded onto a Q-sepharose column (10 ml) equilibrated with Buffer H with 0.1 M NaCl. The bound proteins were eluted with a 9.6 CV gradient of 0.1-0.6 M NaCl gradient in Buffer H. Fractions containing RPA were pooled and loaded onto an ssDNA agarose column (10 ml) equilibrated Buffer H with 0.15 M NaCl. The column was washed successively with 3 CV each of Buffer H with 0.1 M and 0.75 M NaCl, and RPA was eluted with 1.5 CV Buffer H containing 1.5 M NaCl, 50% (v/v) ethylene glycol. The eluate was diluted four-fold with Buffer H with 0 M NaCl and loaded onto a hydroxylapatite column (1.6 ml; Type I, Bio-Rad). The column was washed successively with 5 CV of Buffer H with 0.1 M NaCl, and 10 CV of Buffer AK with 20 mM KPO_4, and RPA was eluted with 5 CV of Buffer AK with 100 mM KPO_4. The peak fractions (200µl) were pooled and purified by a glycerol gradient sedimentation and stored as PCNA.

Preparation of gapped-DNA beads

Cfr10I-digested ends of 30 µg of 2.7 kb pUC19GAP1 (Sun et al., 2014) were biotinylated by incubation with 33 µM biotin-dCTP (PromoKine), 33 µM dGTP and 2 units of Klenow fragment (Clontech) in a 75 µl Klenow reaction mixture [10 mM Tris-HCl (pH 7.5), 7 mM $MgCl_2$, 0.1 mM DTT] at 37°C for 1 h. A gapped structure was introduced to this DNA using two Nt.BbvCI nicking endonuclease sites flanking 38 nt distance. The linearized DNA was treated with 10 units of Nt.BbvCI (NEB) at 37°C for 1 h, then heated at 80°C for 1 min followed by sepharose CL-4B chromatography (1.6 ml, GE Healthcare) in TE containing 0.1 M NaCl. The gapped DNA was eluted in the excluded fractions and the short ssDNA from the gapped region was in the included fraction. The prepared gapped DNA (3 µg) was mixed with 500 µg of Dynabeads M-280 streptavidin (Life Technologies) in 100 µl of BW buffer at RT for 1 h, and gapped-DNA beads bound with ~2 µg of DNA were obtained.

Incorporation of ddAMP at the 3′ end of the gap (Figure 11) was achieved by incubation of 3.6 µg of gapped DNA in a 70 µl Klenow reaction mixture with 4 units of Klenow fragment, 140

μM each of TTP, dCTP and ddATP (GE Healthcare) on ice for 2 h, followed by addition of 5 μl of 0.5 M EDTA. The DNA was conjugated with Dynabeads M-280 streptavidin as above.

Preparation of oligo-DNA beads

Biotinylated 90 mer-oligonucleotide BTN3 was obtained from Sigma Genosys. BTN3 was annealed with BTN30 or BTN28 at a 1:2 ratio as described previously (Waga and Stillman, 1998a), resulting in 3′ and 5′ recessed (3′/5′) or 3′ recessed (3′) primer-template DNAs. Similarly, BTN5 was annealed with BTN32, resulting in 5′ recessed primer-template DNA (5′) (see Table 1 for primer sequences). Oligo-DNA beads were prepared by binding 100 pmol of biotinylated ssDNA (ss) or primer-template DNAs with 50 μl of streptavidin agarose ultra-performance beads (Solulink) in BW buffer (Figure 6A).

PCNA loading

Gapped-plasmid-DNA beads containing 15 ng of DNA were suspended in 10 μl of reaction mixture [10 mM Hepes-NaOH (pH 7.8), 0.05% (v/v) Tween 20, 10 mM $MgCl_2$, 0.2 mM EDTA, 0.01% (w/v) BSA and 0.5 mM DTT] containing 2 mM ATP, 6.2 pmol of PCNA and additional components as indicated. Assays in Figure 3B and C included additionally 40 mM creatine phosphate and 250 ng of creatine-phosphate kinase. The DNA beads were incubated at 32°C for 30 min after addition of the indicated components for loading, and free proteins were removed by four washes with 100 μl of 1xHBS [10 mM Hepes-NaOH (pH 7.8), 3.2 mM EDTA, 0.05% (v/v) Tween20 and 0.15 M NaCl]. The assay with oligo-DNA beads was carried out similarly, except for using of DNA beads with 500 fmol of oligonucleotides and 4.2 pmol of RPA for loading and five washes of 500 μl of 1xHBS after the reaction.

DNA polymerase assay with dA/dT

DNA synthesis reaction was performed in 5 μl of a mixture containing 30 mM Hepes-NaOH (pH7.8), 7 mM $MgCl_2$, 0.01% BSA, 50 μM [α-^{32}P] TTP (Perkin Elmer), 0.5 mM DTT and 200 pmol dA/dT and indicated amounts of DNA polymerases at 37˚C for 15 min. Incorporated TMP into was determined by adsorption of the products to DE81 paper (Whatman) followed by Cherenkov counting with liquid scintillation counter (Beckman).

Labeling of primer DNA

10 pmol of ssDNA primer was labeled with [γ-^{32}P]ATP (Perkin Elmer) using T4 polynucleotide kinase (TAKARA) in 10 μl reaction mixture at 37˚C for 1 h and purified by phenol-chloroform extraction and ethanol precipitation. The labeling efficiency of primer was measured by adsorption to DE81 paper as above.

Exonuclease assay

5 µl of loading buffer containing 80 fmol ^{32}P-TEMP60, 30 mM NaCl, and indicated amounts of p261N was incubated at 37˚C for 10 min. The reaction was stopped by addition of 1 µl of 10 x sample buffer (TAKARA) containing SDS and the product was electrophoresed in 10% polyacrylamide gel with TAE. The gel was fixed in 40% (v/v) methanol, 20% (v/v) acetic acid for 5 min followed by washing with water for 5 min and gel-drying on 3MM paper (Whatman) under vacuum, and the radiolabeled DNA was visualized by autoradiography with FLA-7000 (GE Healthcare).

Site-specific DNA photo-crosslinking

To prepare 3′ end-labeled oligonucleotide substrates for photo-crosslinking, 45 pmol of RF-30 primer was annealed with 30 pmol of TEMP90-R to create AP-Junction or with 30 pmol of TEMP90-Rneo to create AP-End, and incubated with 3.1 µM [α-^{32}P]TTP (PerkinElmer Life Sciences), 20 µM α-S-dCTP (ChemCyte) and 4 units of Klenow fragment at 10°C for 30 min in a 20 µl Klenow reaction mixture, followed by a chase with 50 µM TTP at 10°C for 30 min. After phenol–chloroform (1:1) extraction, the product DNA was incubated with 2.1 nmol of azidophenacyl bromide (APB; Sigma) in a 50 µl volume for 3 h at room temperature in the dark. After removal of unreacted reagent by ethanol precipitation with ethachinmate (NIPPON GENE), the product DNA was dissolved in TE at 50 nM (calculated from the estimated recovery from incorporated TMP), and stored at 4°C in the dark.

Photo-crosslinking oligonucleotide substrate labeled at a fixed position on the template strand was prepared by extension of RF64 on BTN3; 300 pmol of RF64 primer was annealed with 150 pmol of BTN3 and bound to 5 µl of streptavidin agarose ultra-performance beads. The DNA beads were incubated in a 25 µl of Klenow reaction mixture with 4 µM [α-^{32}P]TTP, 24 µM α-S-dCTP and 2 units of Klenow fragment at 10°C for 30 min. After three washes with BW buffer and one wash with TE, the attached RF64 was completely elongated with 250 µM dNTP and 2 units of Klenow fragment at 10°C for 30 min in a 20 µl Klenow reaction mixture. Free nucleotides and proteins were removed by two washes with BW buffer; then the elongated RF64 strand was eluted twice with 50 µl of 0.1 M NaOH. The eluted sample was neutralized by addition of 10 µl of 1 M Tris-HCl (pH 8.0) and 10 µl of 10-fold diluted HCl and reacted with 2.1 nmol of APB in a 130 µl reaction mixture, as above. Aliquots of the product were annealed at 1:1.5 ratio with RF21–RF56 oligonucleotides (Table 1) in TE containing 0.1 M NaCl, and stored at 4°C in the dark.

A 10 µl reaction mixture in a 1.5 ml test tube containing 25 fmol of labeled

oligonucleotide substrate, 60 mM NaCl and additional components as indicated was incubated at RT for 10 min and irradiated with 8 W ultraviolet (UV) C for 5 min at a 10 cm distance from the light source in a UVC 500 Ultraviolet crosslinker (GE Healthcare). The crosslinked DNA–protein complexes were further treated with 5 units of TurboNuclease (Accelagen) for 1 h at RT, and proteins conjugated with labeled nucleotides were separated by SDS-PAGE and autoradiographed as above.

Electrophoretic-mobility-shift assay (EMSA) after glutaraldehyde fixation

As the assay substrates, AP-Junction DNA obtained as described above was further extended at their 3′ end with ddAMP or dAMP, and a dd-Junction and a d-Junction were prepared, respectively (Figure 12A). The 25 fmol substrate was incubated in 5 µl of reaction mixture containing 60 mM NaCl and proteins at RT for 10 min and treated with 0.5 µl of 10% (v/v) glutaraldehyde for 5 min. The crosslinked sample was supplemented with 0.5 µl of electrophoretic-mobility-shift assay (EMSA) loading solution [100 mM Tris-HCl (pH 8.0), 20% (w/v) sucrose, 1 mg/ml bromophenol blue] and separated on a 5% polyacrylamide gel in TAE buffer [20 mM Tris-acetate (pH 7.8), 1.25 mM EDTA] at RT. The shifted DNA was visualized by autoradiography as above.

Holoenzyme assay with Polδ and Polε

A singly-primed template DNA was prepared by annealing M13mp18 ssDNA (TAKARA) to 3-fold molar excess amount of TEMP90-R. The template DNA (30 ng) was then incubated in a 10 µl reaction mixture containing 25 mM Hepes-NaOH (pH 7.8), 10 mM Mg-acetate, 60 mM NaCl, 2 mM ATP, 0.01% (w/v) BSA, 0.5 mM DTT, 10 µM dNTP, [α-^{32}P]TTP and indicated amounts of proteins at 32°C for 30 min. The product DNA was precipitated with ethanol, dissolved in 5 µl alkaline electrophoresis solution [0.3 M NaOH, 2 mM EDTA, 5% (w/v) Ficoll] followed by electrophoresis in a 0.8% alkaline agarose gel at 40 V for 5 hours, and the products were visualized by autoradiography as above.

RESULTS

PCNA loading with CTF18-RFC and its stimulation by addition of Polε

To examine quantitatively PCNA-loading activity by CTF18-RFC, magnetic beads were conjugated with 2.7 kb dsDNA to prepare the substrate DNA in pseudo-circular situation as described in *Preparation of gapped DNA beads* (Figure 2A, Sun et al., 2014). This DNA harbored a 38 nt-gapped region to generate 3′ primer-template junction where CTF18-RFC would target to load PCNA. Indeed, DNA beads-retained PCNA was observed according to the amounts (20-60 fmol) of CTF18-RFC only in the presence of ATP (Figure 2B, lanes 2-8). The ATP-dependent manner represented that the retained PCNA was the result of PCNA loading by CTF18-RFC. I quantified the PCNA band intensities and estimated that 2.4 PCNA trimer molecules were loaded to a substrate DNA molecule with 60 fmol of CTF18-RFC.

Next, in order to investigate the functional significance of the interaction between CTF18-RFC and Polε, I examined the effect of Polε for PCNA loading by CTF18-RFC along with another replicative DNA polymerase Polδ as a negative control, which does not interact with CTF18-RFC. Neither Polε nor Polδ alone exhibited any PCNA loading (Figure 3A, lanes 6, 10). Addition of Polε to CTF18-RFC resulted in 3-5 fold augmentation of the PCNA loading (lanes 2–9). The augmentation was not observed with Polδ (lanes 10-13), indicating that Polε specifically augments PCNA loading reaction by CTF18-RFC. The N-terminal half of Polε p261 (p261N), carrying the region necessary for interaction with CTF18-RFC (Murakami et al., 2010), showed similar stimulation (Figure 3B, lanes 7–9). PCNA loading was also examined with two other loader complexes, the canonical PCNA loader RFC and CTF18-RFC(5), the pentameric derivative of CTF18-RFC lacking DCC1 and CTF8. Neither RFC nor CTF18-RFC(5) interacts stably with Polε (Murakami et al., 2010). In the absence of p261N, PCNA loading activity was nearly the same with RFC, CTF18-RFC and slightly lower with CTF18-RFC(5) at 30 mM NaCl (Figure 3C, lanes 2–7). In the presence of p261N, only CTF18-RFC exhibited enhanced PCNA loading (Figure 3C, lanes 8–13), indicating that the specific interaction of CTF18-RFC with Polε is important to augment PCNA loading by CTF18-RFC.

Polε stimulates loading of PCNA by CTF18-RFC under near-physiological conditions

CTF18-RFC has been reported to be less active for PCNA loading than RFC, reflecting higher salt sensitivity of ssDNA-stimulated ATPase and binding to 3′ primer-template junction DNA in CTF18-RFC than in RFC (Bermudez et al., 2003). Therefore, the effects of salt concentration on PCNA loading were examined. RFC and CTF18-RFC loaded similar amounts

of PCNA at 30 mM NaCl condition. PCNA loading by RFC increased as the NaCl concentration increased, whereas PCNA loading by CTF18-RFC decreased with increasing NaCl and was very low at near-physiological salt concentrations over 100 mM NaCl (Figure 4A). However, in the presence of p261N, significant PCNA loading was observed even at 100 mM NaCl (Figure 4B). Active PCNA loading by CTF18-RFC at physiological salt concentrations requires interaction with Polε.

ssDNA binding protein RPA is involved in various DNA metabolic reactions including DNA replication and repair (Fanning et al., 2006). It is expected that presence of RPA in the PCNA loading reaction would make it more physiological. When I added 42.5 and 85 fmol of RPA in PCNA loading reaction with 16 fmol of the gapped DNA by CTF18-RFC alone at 60 mM NaCl, less PCNA was loaded than without RPA (Figure 4C, lanes 3-5). This result is consistent with a previous report with *S. cerevisiae* Ctf18-RFC that saturating amounts of RPA inhibit the PCNA loading (Bylund and Bergers, 2005). In the presence of Polε, however, PCNA loading by CTF18-RFC was maintained or slightly increased even with RPA (Figure 4C, lanes 6-8). Collectively, these data indicate that at near-physiological conditions. i.e., in the presence of RPA and a higher salt, CTF18-RFC can load PCNA after it has formed a complex with Polε.

The CTF18-RFC–p261N complex loads PCNA efficiently through cooperative DNA binding

Polε has intrinsically high affinity for various DNA structures, while Polδ uses its high affinity to PCNA to access to a template DNA (Chilkova et al., 2007). This led me to hypothesize that CTF18-RFC might be recruited to its target site through its interaction with DNA-bound Polε. Therefore, protein binding to gapped DNA beads was analyzed during PCNA loading (Figure 5). p261N bound to the gapped DNA in the absence of other proteins, and addition of PCNA did not affect this binding (Figure 5A, lanes 2, 3). Similar DNA binding was observed with Polε, but not Polδ, even with PCNA (Figure 5B and C, lanes 2, 3). CTF18-RFC alone bound to DNA at a very low level, and a limited PCNA loading occurred (Figure 5A-C, lanes 4, 5). When p261N was present, >10% of the input CTF18-RFC was retained on the DNA with or without PCNA, and 3-fold more PCNA was loaded than in the absence of p261N (Figure 5A, lanes 6, 7). Similarly, increased CTF18-RFC retention and PCNA loading were observed with Polε, but not Polδ (Figure 5B, C lanes 6, 7). Notably, about 2-fold greater binding of p261N and Polε to DNA occurred in the presence of CTF18-RFC than in its absence (Figure 5A, B lanes 2, 3, 6, 7). These results indicated that CTF18-RFC and p261N/Polε bound to DNA cooperatively. Thus,

CTF18-RFC could access target DNA through the cooperative binding, which would further lead to enhanced PCNA loading at near physiological salt concentrations.

PCNA loading by the CTF18-RFC–p261N complex occurs at 3′ primer-template junctions

Because CTF18-RFC is able to support PCNA-dependent DNA synthesis by Polδ (Bermudez et al., 2003, Shiomi et al., 2004), 3′ primer-template junctions are considered as a target structure for PCNA loading by CTF18-RFC. However, PCNA loading by the CTF18-RFC–p261N/Polε complex would be possibly a novel mechanism, I studied the target DNA structures for PCNA loading. Prior to the experiments, I prepared p261N^{exo-}, in which the highly conserved Asp275 of the exonuclease motif of B-family polymerases (Henninger and Pursell, 2014) was substituted with alanine to avoid degradation of substrate DNAs during experiments. Purified p261N^{exo-} did not exhibit any detectable nuclease activity (Figure 6A), and augmented PCNA loading by CTF18-RFC slightly more effectively than p261N (Figure 6B), indicating that the substitution did not affect the stimulation.

RFC targets 3′ primer-template junctions to load PCNA (Ellison and Stillman, 2003). The target DNA of PCNA loading by CTF18-RFC and the CTF18-RFC–p261N/Polε complex were analyzed with various DNA structures, which were attached to agarose beads (Figure 7A). PCNA loading by CTF18-RFC was observed with 3′ and 5′ recessed primer-template DNA (3′/5′) only in the presence of RPA, which prevents PCNA from sliding off the DNA ends (Figure 7B). Among ssDNA (ss), 3′ and 5′ recessed (3′/5′), 3′ recessed (3′), and 5′ recessed primer-template DNAs, CTF18-RFC alone in the presence of ATP loaded PCNA onto 3′/5′ and 3′ DNAs (Figure 7C, lanes 5, 8). Thus, CTF18-RFC, like RFC, specifically loads PCNA at 3′ primer-template junctions. In the presence of p261N^{exo-} and ATP, increased PCNA loading was observed specifically with 3′/5′ and 3′ DNAs (Figure 7C, lanes 7, 10), but not with ss (lane 4). Small amount of PCNA were detected with 5′ DNA (lanes 12, 13) in the presence of p261N^{exo-} and even in the absence of ATP. This could be due to p261N^{exo-}-mediated binding of PCNA to DNA not to direct loading of PCNA onto DNA. In the absence of ATP, both CTF18-RFC and p261N^{exo-} bound non-specifically to all the DNA structures that were tested (lanes 3, 6, 9, 12, Figure 7D). Notably, in the absence of other proteins, p261N^{exo-} showed dose-dependent, and high affinity binding to several DNA structures (Figure 7E), implying that p261N^{exo-} could be the dominant cause of this non-specific DNA binding. In the presence of PCNA and ATP, bindings of CTF18-RFC and p261N^{exo-} to DNA with 3′ primer-template junctions increased (Figure 7C, lanes 7, 10), whereas binding to other structures decreased (Figure 7C, lanes 4, 13 and Figure 7D), compared with the

absence of ATP. Thus, the cooperative action of CTF18-RFC and p261N^{exo-} could increase specificity for 3′ primer-template junctions during PCNA loading.

Analysis of binding modes of RFC to a 3′ primer end by photo-crosslinking

It has been demonstrated that DNA-bound Polε recruits CTF18-RFC to DNA, and they bind to cooperatively on the DNA and load PCNA at the site. DNA polymerases bind to 3′ primer-template junctions to elongate primer DNA. Thus, both CTF18-RFC and Polε can recognize 3′ primer-template junctions during the PCNA loading. How does they share the same binding DNA when they are in a complex? To identify which protein subunit directly interacts with the target DNA during PCNA loading, site-specific DNA photo-crosslinking analysis with APB was employed (Yang and Nash, 1994, Lagrange et al., 1996, Lee and Bell, 1997). This reagent couples with the thiol group of S-dNMP in a substrate DNA (Figure 8A). The substrate "AP-Junction" had AP coupled to a 3′ primer-template junction along with the next ^{32}P-labeled nucleotide (Figure 8B). After UV-irradiation and nuclease treatment, proteins most proximal to the AP-labeled nucleotides during a defined period of UV irradiation can be detected as ^{32}P-labeled bands by electrophoresis (Figure 8C). Therefore, a band of higher intensity will have a higher probability of being attached to the target site than a band of lower intensity.

When I examined RFC and AP-Junction at 60 mM NaCl without nuclease treatment, a high-molecular-mass smear and one or two bands migrating slower than the raw RFC1 and RFC2–5 peptides were detected only after UV-irradiation (Figure 8D, lanes 2–7). After nuclease digestion, signal intensities were decreased in general and bands corresponding to RFC2–5 became prominent in the presence of ATPγS (Figure 8D, lanes 8–10). Thus, RFC2–5 are the major docking protein when ATP-bound RFC is associated with the 3′ primer-template junction. Addition of PCNA in the presence of ATP enhanced the RFC1 signal (Figure 8D, lane 12), and the RFC2–5 signals increased in the presence of ATPγS (Figure 8D, lane 13). These results represent two binding modes of RFC to the 3′ primer-template junction. One is via RFC2–5 bound by ATP (an ATPγS plus condition). The other is via RFC1 in the presence of PCNA on the DNA. These signals were specific for the 3′ primer-template junction, because moving the target 3′ primer end to a double-stranded end decreased most of the signals ("AP-End"; Figures 8B and D, lanes 14–16). The molecular mass of labeled protein could not be determined precisely with this assay, so the specific subunits of RFC2–5 that bound to 3′ primer end could not be distinguished.

Analysis of binding modes of CTF18-RFC and p261N^{exo-} to 3′ primer ends

As representing weak PCNA loading activity of CTF18-RFC, its binding to a 3′ primer end at 60 mM NaCl was hardly detectable even with PCNA and ATPγS (Figure 9A, lanes 1–3). At 10 mM NaCl in the presence of ATPγS and PCNA (lane 9), however, a similar binding profile was observed for CTF18 and RFC2–5 as was seen with RFC, though only limited bindings occurred with ATP and PCNA or without PCNA (lanes 4–8). This result indicated that binding of CTF18-RFC to a 3′ primer end only occurred in the intermediate state of PCNA loading, and that binding in the ATP-bound state without PCNA, or after PCNA loading and ATP hydrolysis was less stable than the binding seen with RFC, demonstrating the weak intrinsic DNA binding of CTF18-RFC.

When p261N^{exo-} was added to the experiments, it showed a much greater level of binding to a 3′ primer end than CTF18-RFC (Figure 9B, lanes 2, 3). Addition of p261N^{exo-} and CTF18-RFC together in the presence of PCNA and ATPγS, representing a condition of the PCNA-loading intermediate, increased bindings of both p261N^{exo-} and CTF18-RFC to DNA. About 3-fold more p261N^{exo-} and 5-fold more CTF18 bound to a 3′ primer end than when they were included individually (Figure 9C), demonstrating their cooperative binding as in the DNA pull-down assay (Figure 5). Again, this stimulation of the DNA binding depended on their specific interaction, as CTF18-RFC(5) did not exhibit any significant increase (Figure 9B, lane 6).

Even when p261N^{exo-} and CTF18-RFC bound to DNA cooperatively in the presence of PCNA and ATPγS, the signal of CTF18 binding was <5% of the p261N^{exo-} signal, indicating that the 3′ primer end was mostly occupied by p261N (Figure 9B, lane 4, Figure 9D, lane 3). In the presence of ATP or the absence of nucleotides to minimize the level of the intermediate state of PCNA loading, the ratio of binding signal of CTF18 to p261N was decreased to a half (Figure 9D). Thus, p261N attaches mostly with a 3′ primer end and CTF18-RFC is tethered by the p261N. Then, temporal access of CTF18-RFC to a 3′ primer end will occur for loading of PCNA.

Analyses of the binding modes of CTF18-RFC and p261N^{exo-} on the template strand at primer-template junctions

The binding of CTF18-RFC and p261N^{exo-} on the template strand at primer-template junctions were investigated with a 90-mer ssDNA labeled with ^{32}P-TMP and AP-crosslinker through S-dCMP at positions 25 nt and 26 nt from the 3′ end, respectively (AP-Template, Figure 10A). Six primers, from 21 nt to 41 nt, were annealed at the 3′ end side of the 90 mer to make six constructs in which the position of the AP-crosslinker relative to the 3′ primer end (single–double-strand junction) varied from −5 (ssDNA region) to +20 (double-stranded-DNA region)

(Figure 10B).

Binding profiles of p261N^{exo-} and CTF18-RFC in the presence of PCNA and ATPγS were studied with the six AP-Template substrates. p261N^{exo-} was crosslinked to the AP obviously when it was in positions −5 to +15, whereas CTF18-RFC crosslinked to AP only in positions −5 and ±0 (Figure 10C, lanes 2–7 and 9–14). In assays containing both p261N^{exo-} and CTF18-RFC (Figure 10C, lanes 16–21), increased bindings of both proteins were observed, corresponding to 3′ primer-template junctions-specific binding of CTF18, and cooperative DNA binding of the CTF18-RFC–Polε complex. The binding of CTF18 at position −5 corresponded to ~25% of the signal for binding of p261N^{exo-}, indicating that the association of CTF18-RFC with the template strand at this point (relative to that of p261N^{exo-}) was greater than the association with the 3′ primer end (Figure 9B). The prominent binding of CTF18 at −5 and ±0 in the presence of ATPγS was not observed in the presence of ATP (Figure 10D), where the level of the intermediate state of PCNA loading should be low as described above. Thus, in the presence of ATPγS, the greater association of CTF18 with the region from the single–double-strand junction to the ssDNA template strand suggests a temporal association of CTF18-RFC to the region during PCNA loading.

PCNA loading by CTF18-RFC–Polε is blocked if Polε is in the DNA-synthesis mode

All the preceding experiments were carried out without dNTPs, so demonstrated with Polε in a DNA non-synthesizing mode. To investigate the interactions with Polε in a DNA-synthesis mode, I prepared a primer-template junction substrate with dideoxynucleotide (ddNMP) at the 3′ primer end (deoxidized 3′ primer end, Figure 11A). In the presence of this substrate and the next-incoming dNTP, Polε would be trapped in the act of extending DNA with deoxynucleotides (a DNA-synthesis mode), as demonstrated by a structural study of yeast Polε (Hogg et al., 2014). Indeed, discrete bindings of Polα and Polδ to a similar substrate DNA was observed only in the presence of the incoming dNTP (Tsurimoto and Stillman, 1991). To test the DNA-synthesis mode of Polε at the deoxidized 3′ primer end, a ^{32}P-labelled primer-template DNA substrates with incorporated ddAMP or dAMP at its 3′ end were prepared (“dd-Junction” “d-Junction”, Figure 11A). When this substrate was incubated with Polε^{exo-} in the presence of TTP, the next incoming nucleotide, stronger shifted bands were observed than without TTP (Figure 11B, lanes 5, 6) or with a substrate lacking the deoxidized 3′ primer end (lanes 2, 3). This result demonstrated a strategy to produce Polε^{exo-} in synthesizing mode on a substrate DNA.

On the basis of Figure 11 that addition of next incoming nucleotide can control DNA

binding modes of Polε at the deoxidized 3′ primer end, gapped-DNA beads with ddAMP at the 3′ primer end of gap were prepared (Figure 12A), to examine the effect of dGTP, the incoming nucleotide, on PCNA loading by CTF18-RFC in the presence of Polε^{exo-}. dGTP did not affect PCNA loading by CTF18-RFC alone in the presence of ATP (Figure 12B, lanes 3, 8), but it suppressed the stimulation of PCNA loading by the addition of Polε^{exo-} (Figure 12B, lanes 4–6, 9–11). This result indicates that Polε^{exo-} in the DNA synthesizing mode does not augment PCNA loading as well as Polε^{exo-} in the non-DNA synthesizing mode.

Assembly of the CTF18-RFC and PCNA with Polε in DNA-synthesis mode

By the same EMSA assay, binding of RFC to a 3′ primer-template junction was observed in the presence of PCNA and ATPγS (Tsurimoto and Stillman, 1991). However, DNA binding of CTF18-RFC by the same method was not detected even with PCNA and ATPγS (Figure 11C, lanes 2–4). This difference between two loaders demonstrates again the relatively low affinity of CTF18-RFC for DNA. I examined the effects of PCNA and CTF18-RFC on the mobility of the Polε^{exo-}-DNA band appeared in synthesizing mode. The band was slightly supershifted by the addition of PCNA (Figure 11C, lane 10), representing the formation of a Polε^{exo-}–PCNA complex on the DNA. In this case, PCNA was spontaneously entrapped from the free end of DNA in the absence of clamp loaders (Burgers and Yoder, 1993). Addition of CTF18-RFC to Polε^{exo-} supershifted the Polε^{exo-} band (Figure 11C, lane 8), indicating that CTF18-RFC is tethered to Polε in synthesizing mode at the 3′ primer end. Addition of PCNA to CTF18-RFC and Polε^{exo-} produced a 2-fold to 3-fold increase in intensity of the supershifted band, compared with no PCNA (Figure 11C, lane 12), suggesting the presence of a stable assembly of Polε^{exo-}–CTF18-RFC including PCNA on the dd-Junction substrate. By addition of CTF18-RFC(5) instead of CTF18-RFC, the supershifted band could not be observed, indicating that the complex formed via the specific interaction of CTF18-RFC and Polε (Figure 11D). Note that all shifted bands were observed in the presence of TTP, indicating that these complexes formed on Polε^{exo-} in synthesizing mode.

DNA synthesis by CTF18-RFC–Polε–PCNA

The trimeric assembly of CTF18-RFC–Polε–PCNA forms at the 3′ primer-template junction when Polε is synthesis mode. To study DNA synthesis by this assembly, I performed a holoenzyme assay with CTF18-RFC, Polε, PCNA and RPA using a singly primed M13mp18 as template DNA. Efficient DNA synthesis was observed with them (Figure 13A, lane 5). Omission of one of the components resulted in the severe or total loss of DNA synthesis except for when

RPA was omitted (lanes 1–4); in this case, DNA products with a size of about 1.5 kb accumulated. Thus, efficient initiation of DNA synthesis occurred with the trimeric complex, and RPA was further required for DNA elongation, probably by its ability to resolve secondary structures on the template DNA. A decrease in the amount of CTF18-RFC resulted in reduced DNA synthesis, but the mean-product-lengths were not affected significantly (lanes 5–7), suggesting that CTF18-RFC might be required for the efficient initiation of DNA synthesis by Polε.

To determine whether the specific assembly of CTF18-RFC–Polε–PCNA mediates the efficient DNA synthesis, I compared DNA syntheses with Polδ and Polε in the presence of RPA in reactions where PCNA was loaded by either RFC or CTF18-RFC. Similar to previously published results (Bermudez et al., 2003, Shiomi et al., 2004), Polδ synthesized DNA efficiently with PCNA loaded by RFC, but less efficiently with PCNA loaded by CTF18-RFC (Figure 13B, lanes 10–15). This difference might reflect the difference in the efficiency of PCNA loading by these two loaders. PCNA loaded by RFC also stimulated the DNA synthesis by Polε via the previously reported interaction between Polε and PCNA (Chilkova et al., 2007, Bermudez et al., 2011, lanes 3–5). Interestingly DNA synthesis in the presence of CTF18-RFC was more efficient and produced longer DNA than in the presence of RFC (lanes 6–8). Collectively, these results suggest that CTF18-RFC is more adapted as a PCNA loader for Polε than RFC and vice versa for Polδ. The CTF18-RFC–Polε–PCNA complex synthesized DNA more processively than Polε in the presence of PCNA loaded by RFC, suggesting that it functions as a genuine functional DNA polymerase holoenzyme.

DISCUSSION

CTF18-RFC complexed with Polε actively loads PCNA

The intrinsic PCNA loading activity of CTF18-RFC was almost inactive under near-physiological conditions. However, the activity was restored if CTF18-RFC was present in the complex with Polε (Figure 4), indicating that CTF18-RFC functions as an active PCNA loader when CTF18-RFC is associated with Polε. Although there is a little controversy (Johnson et al., 2015, Burgers et al., 2016), it is widely accepted that Polε is the major leading-strand DNA polymerase (Purcell et al., 2007, Nick McElhinny et al., 2008, Yu et al., 2014, Georgescu et al., 2014 and 2015a, Daigaku et al., 2015, Yeels et al., 2017). Therefore, CTF18-RFC can be expected to be one of functional components in the replisome, especially on the leading strand. Cell-biological studies have demonstrated that CTF18 surely accumulates in the S phase chromatin (Shiomi et al., 2012), localizes at the replication fork (Sirbu et al., 2013, Alabert et al., 2014, Dewar et al., 2017), and is co-purified with CMG helicase from worm embryo extracts (Soonevile et al., 2017). In addition, dysfunction of CTF18-RFC impairs the normal progression of the replication fork in human cells (Terett et al., 2009), and decreases the localization of PCNA in the S-phase chromatin in *S. cerevisiae* (Lengronne et al., 2006, Kubota et al., 2011). Thus, CTF18-RFC complexed with Polε will function as an active PCNA loader in the eukaryotic replisome. Under certain conditions, however, Polδ is able to replace function of Polε in leading-strand synthesis (Tsurimoto et al., 1990, Miyabe et al., 2015, Yeels et al., 2017). In this condition, CTF18-RFC might not be required for an active PCNA loader.

A recent structural study suggests that the interaction of Ctf18-Dcc1-Ctf8 module to Polε occurs without any post-translational modifications and does not inhibit the DNA binding of Polε for its DNA synthesis (Grabarczyk et al., 2018). The result of EMSA assay in Figure 11B, which showed that CTF18-RFC bound to Polε in DNA synthesis mode, agrees with this notion that CTF18-RFC will be associated with Polε throughout DNA replication. In addition, since their interaction was observed independently on the cell-cycle (García-Rodríguez et al., 2015), the CTF18-RFC–Polε complex would have additional roles out of DNA replication, for example, in nucleotide-excision repair reactions (Ogi et al., 2010) and in telomere maintenance pathways (Hiraga et al., 2006, Gao et al., 2014, Khair et al., 2010).

DNA binding of the CTF18-RFC–Polε complex

Cooperative DNA binding of CTF18-RFC and Polε (p261N) was observed in various assays, though Polε (p261N) binds to DNA more strongly than CTF18-RFC. p261N bound to

DNA in a fairly non-specific manner, which consequently directed the CTF18-RFC–p261N complex to any structured DNAs. Importantly, the complex became more specific to the 3′ primer-template junction structures under PCNA-loading conditions (Figure 7), indicating that the process of PCNA loading or involvement of PCNA to the complex may exhibit specific binding to the 3′ primer-template junction. DNA photo-crosslinking experiments demonstrated that, in the complex of CTF18-RFC–p261N, p261N was associated predominantly with the junction and association of CTF18-RFC to the sites was minor and became detectable in the PCNA-loading intermediate condition (Figures 9, 10), although evidently sufficient for PCNA loading. PCNA loading by CTF18-RFC–Polε was suppressed when Polε was in DNA-synthesis mode at the 3′ primer-template junction, whereas efficient PCNA loading occurred with the Polε in non-synthesizing mode (Figure 12B). Since Polε occupies a large portion of a primer-template junction DNA in DNA synthesis mode as indicated their co-crystal structure (Hogg et al., 2014), the CTF18-RFC complexed with Polε will be hardly accessible with the 3′ primer-template junction in its DNA-synthesis mode. Thus, switching of DNA-synthesis modes of Polε could be an essential part of the mechanism for PCNA loading by CTF18-RFC.

CTF18-RFC maintains DNA synthesis of Polε via its PCNA loading

As I demonstrated with RPA and primed M13mp18 DNA as a template (Figure 13B), DNA synthesis with two DNA polymerases could be stimulated by PCNA, once loaded by any loaders. Without specific interaction between DNA polymerases and loaders, PCNA stimulates both DNA polymerase according to the loading efficiency to DNA and affinity between PCNA and DNA polymerase. Importantly, Polε synthesized much longer DNA with PCNA loaded by CTF18-RFC than RFC (Figure 13B, lanes 3–8). The loaded PCNA will be captured by the CTF18-RFC–Polε complex and involved in the novel assembly (Figure 11B, D), which is responsible for efficient and processive DNA synthesis by Polε. Thus, the assembly of CTF18-RFC–Polε–PCNA will be one of functional statuses of the Polε holoenzyme in the replication fork. Of the three replicative DNA polymerases, Polα and ε are tethered to the CMG helicase while Polδ is not (Gambus et al., 2009, Sengupta et al., 2013, Sun et al., 2015). Similarly, CTF18-RFC co-localizes with CMG helicase but RFC does not (Dewar et al., 2017, Sonneville et al., 2017). These studies suggest that at the replication fork, Polε and CTF18-RFC act processively following progression of CMG helicase for leading-strand synthesis, while RFC and Polδ act distributively for lagging-strand synthesis (Masuda et al., 2007, Kang et al., 2012, Yu et al., 2014, Georgescu et al., 2014 and 2015a).

A model of actions of the CTF18-RFC–Polε complex in the replisome

I demonstrated that CTF18-RFC complexed with Polε loads PCNA to maintain its DNA synthesis. Based on this result, I propose a model of actions of the CTF18-RFC–Polε complex in the replisome (Figure 14). The leading-strand replisome core consists of CMG helicase, Polε and additional CMG-associating factors such as TIM/TIPIN and CLASPIN (Csm3/Tof1 and Mrc1 in *S. cerevisiae*). CTF18-RFC will be involved in the complex by association with Polε. During elongation phase, previously loaded PCNA maintains efficient Polε-catalyzed leading-strand synthesis [Yeeles et al., 2017; Figure 14, (i) Synthesizing]. If the replication fork proceeded at a normal rate, Polε maintaining a complex with CMG would remain in DNA-synthesis mode, and the CTF18-RFC tethered to Polε would have little opportunity to access the 3′ primer-template junction. By physical obstacles or by stochastic reasons (Lopes et al., 2011, Le et al., 2015), Polε will occasionally stall and uncouple from PCNA and other replisome components [(ii) Stalling and Uncoupling], and shift in the DNA non-synthesizing mode. The shift leads to the CTF18-RFC having an opportunity to access the 3′ primer end and load a fresh PCNA at the site [(iii) PCNA loading]. Once PCNA is loaded, the stable CTF18-RFC–Polε–PCNA complex will be formed to restart DNA synthesis [(iv) Synthesis restart], and returned to the original status of as the leading-strand replisome [(i) Synthesizing]. Dysfunction of the CTF18-RFC complex, which would impair the function of the backup system of leading-strand DNA synthesis, would affect the gross replication rate and become sensitive against replication stress, as has been observed in human cells (Terret et al., 2009). Though there have been little experimental evidences showing that PCNA is loaded on leading strand in eukaryotic DNA replication, it was reported that a bacterial replisome stalls stochastically, and successive clamp loading occurs on leading strand to maintain the DNA synthesis (Graham et al., 2017). Thus, the similar active clamp loading on leading strand may occur in eukaryotes.

Importance of CTF18-RFC–Polε for maintenance of PCNA dosage between two sister strands

DNA replication in eukaryotes is not only just duplication of the genetic information but also transmission of chromosomal DNA structure as the epigenetic information to next generation (Bell and Labib, 2016). For this purpose, replicated chromosomes recruit various factors to process replicated DNA molecules, reorganize nucleosomes, and modify DNA and histones. Numbers of PCNA binding proteins functioning for the organization of replicated chromosomes have been identified (Moldovan et al., 2007, Choe and Moldovan, 2017). Loaded

PCNA at the replicated DNA will serve as a landmark of a recently replicated region for these PCNA binding proteins (Georgescu et al., 2015b). RFC loads PCNA on every 3′ end of lagging-strand DNA, which are produced every 150 nt in average (Smith and Whitehouse, 2012), whereas it has been thought that only one PCNA will be loaded for one leading-strand synthesis event (Waga and Stillman, 1998b, Kubota et al., 2013a). This mechanism will produce unequal PCNA distribution between leading- and lagging-strands, in which proper organization of replicated chromosomes via actions of PCNA binding proteins will be hard to explain. However, recent analyses in *S. cerevisiae* (Yu et al., 2014) demonstrated that the ratio of PCNA on the lagging strand to that on the leading strand is only about 2 : 1, which is smaller than the expected ratio on the basis of the number of priming events that occur on the two strands. The authors suggested that the smaller difference of PCNA ratio would be due to its unloading mechanism from lagging strands. My data suggest the alternative mechanism of active PCNA-loading on leading strand, engaged by the CTF18-RFC–Polε complex. This active loading to the leading strand will occur during replication on a routine basis judging form importance of CTF18-RFC to maintain the normal replication rate (Terret et al., 2009). Thus, this mechanism might increase the dosage of PCNA on the leading strand, providing sufficient opportunities for PCNA binding proteins to act.

Consistent with this notion, defects of Ctf18, Dcc1 and Ctf8 affect a wide range of deficiencies in chromosomal-DNA metabolism (Mayer et al., 2001, Hanna et al., 2001, Naiki et al., 2001, Hiraga et al., 2006, Ogiwara et al., 2007, Ansbach et al., 2008, Crabbé et al., 2010, Khair et al., 2010, Kubota et al., 2011, Gellon et al., 2011, Foltman et al., 2013, Gao et al., 2014). For example, Ctf18-RFC, along with the major PCNA unloader Elg1-RFC are implicated as factors required for establishment of sister chromatid cohesion during DNA replication as described in introduction (Mayer et al., 2001, Hanna et al., 2001, Xu et al., 2007, Maradeo and Skibbens, 2009, Parnas et al., 2009, Takahashi et al., 2010, Tong and Skibbens, 2015), without any obvious physical interactions with components of the cohesin complex or factors directly involved in the establishment (Gavin et al., 2002, Murakami et al., 2010, Kubota et al., 2013b). It is thought that cohesin is loaded onto chromatin prior to the DNA replication (Uhlmann and Nasmyth, 1998, Takahashi et al., 2004), and interdependent dynamics occurs between the cohesin and replisome on the replicating chromosome when they encounter (Terret et al., 2009, Kanke et al., 2016). Under this situation, Ctf18-RFC and Elg1-RFC may cooperatively retain PCNA evenly between two sister DNAs, allowing the cohesin acetyltransferese Eco1 to work

properly. Alternatively, the CTF18-RFC–Polε complex may maintain fork progression through the cohesin ring on the parental DNA. Similar fork protection mechanism may occur when the CTF18-RFC–Polε complex encounters DNA damage. In this case, activation of S-phase checkpoint to arrest the cell cycle will be the major outcome.

Taken together, PCNA loading by the CTF18-RFC–Polε complex has two roles for DNA replication. One is to maintain leading-strand synthesis at template DNA structures that disrupt Polε progression, by supplying *de novo* PCNA to restore DNA synthesis. The second role is active PCNA loading to the leading strand through the above mechanism, which balances PCNA dosage between the two DNA strands, enabling PCNA-binding proteins to function similarly on both strands. My biochemical studies have opened the future-lines of studies asking how, when and where the CTF18-RFC–Polε complex will be necessary during DNA replication to elucidate the novel PCNA dynamics.

Reference

Aksenova, A., Volkov, K., Maceluch, J., Pursell, Z. F., Rogozin, I. B., Kunkel, T. A., Pavlov, Y. I. and Johansson, E. (2010) Mismatch repair-independent increase in spontaneous mutagenesis in yeast lacking non-essential subunits of DNA polymerase ε. *PLoS Genet.*, **6**:e1001209.

Alabert, C., Bukowski-Wills, J. C., Lee, S. B., Kustatscher, G., Nakamura, K., de Lima Alves, F., Menard, P., Mejlvang, J., Rappsilber, J. and Groth, A. (2014) Nascent chromatin capture proteomics determines chromatin dynamics during DNA replication and identifies unknown fork components. *Nat. Cell Biol.,***16**, 281-93.

Ansbach, A. B., Noguchi, C., Klansek, I. W., Heidlebaugh, M., Nakamura, T. M. and Noguchi, E. (2008) RFCCtf18 and the Swi1-Swi3 complex function in separate and redundant pathways required for the stabilization of replication forks to facilitate sister chromatid cohesion in Schizosaccharomyces pombe. *Mol. Biol. Cell*, **19**, 595-607.

Araki, H., Hamatake, R. K., Johnston, L. H. and Sugino, A. (1991a) DPB2, the gene encoding DNA polymerase II subunit B, is required for chromosome replication in Saccharomyces cerevisiae. *Proc. Natl. Acad. Sci. USA.,* **88**, 4601-5.

Araki, H., Hamatake, R. K., Morrison, A., Johnson, A. L., Johnston, L. H. and Sugino, A. (1991b) Cloning DPB3, the gene encoding the third subunit of DNA polymerase II of Saccharomyces cerevisiae. *Nucleic Acids Res.,* **19**, 4867-72.

Bae, S. H., Bae, K. H., Kim, J. A. and Seo, Y. S. (2001) RPA governs endonuclease switching during processing of Okazaki fragments in eukaryotes. *Nature*, **412**, 456-61.

Bell, S. P. and Stillman, B. (1992) ATP-dependent recognition of eukaryotic origins of DNA replication by a multiprotein complex. *Nature*, **357**, 128-34.

Bell, S. P. and Labib, K. (2016) Chromosome Duplication in Saccharomyces cerevisiae. *Genetics,* **203**, 1027-67.

Burgers, P. M. and Yoder, B. L. (1993) ATP-independent loading of the proliferating cell nuclear antigen requires DNA ends. *J. Biol. Chem.*, **268**, 19923-6.

Burgers, P. M. J., Gordenin, D. and Kunkel, T. A. (2016) Who Is Leading the Replication Fork, Pol ε or Pol δ? *Mol. Cell,* **61**, 492-3.

Berkowitz, K. M., Sowash, A. R., Koenig, L. R., Urcuyo, D., Khan, F., Yang, F., Wang, P. J., Jongens, T. A. and Kaestner, K. H. (2012) Disruption of CHTF18 causes defective meiotic recombination in male mice. *PLoS Genet.,* **8**:e1002996.

Bermudez, V. P., Maniwa, Y., Tappin, I., Ozato, K., Yokomori, K. and Hurwitz, J. (2003) The alternative Ctf18-Dcc1-Ctf8-replication factor C complex required for sister chromatid cohesion loads proliferating cell nuclear antigen onto DNA. *Proc. Natl. Acad. Sci. USA.,* **100**, 10237-42.

Bermudez, V. P., Farina, A., Raghavan, V., Tappin, I. and Hurwitz, J. (2011) Studies on human DNA polymerase epsilon and GINS complex and their role in DNA replication. *J. Biol. Chem.,* **286**, 28963-77.

Borges, V., Smith, D. J., Whitehouse, I. and Uhlmann, F. (2013) An Eco1-independent sister chromatid cohesion establishment pathway in S. cerevisiae. *Chromosoma*, **122**, 121-34.

Bloom, L. B. (2009) Loading clamps for DNA replication and repair. *DNA Repair,* **8**, 570-8.

Bylund, G. O. and Burgers, P. M. (2005) Replication protein A-directed unloading of PCNA by the Ctf18 cohesion establishment complex. *Mol. Cell. Biol.*, **25**, 5445-55.

Chilkova, O., Jonsson, B. H. and Johansson, E. (2003) The quaternary structure of DNA polymerase epsilon from Saccharomyces cerevisiae. *J. Biol. Chem.,* **278**, 14082-6.

Chilkova, O., Stenlund, P., Isoz, I., Stith, C. M., Grabowski, P., Lundström, E. B., Burgers, P. M. and Johansson, E. (2007) The eukaryotic leading and lagging strand DNA polymerases are loaded onto primer-ends via separate mechanisms but have comparable processivity in the

presence of PCNA. *Nucleic Acids Res.,* **35***,* 6588-97.

Choe, K. N. and Moldovan, G. L. (2017) Forging Ahead through Darkness: PCNA, Still the Principal Conductor at the Replication Fork. *Mol. Cell,* **65**, 380-92.

Crabbé, L., Thomas, A., Pantesco, V., De Vos, J., Pasero, P. and Lengronne, A. (2010) Analysis of replication profiles reveals key role of RFC-Ctf18 in yeast replication stress response. *Nat. Struct. Mol. Biol.,* **17**, 1391-8.

Daigaku, Y., Keszthelyi, A., Müller, C. A., Miyabe, I., Brooks, T., Retkute, R., Hubank, M., Nieduszyski, C.A. and Carr, A. M. (2015) A global profile of replicative polymerase usage. *Nat. Struct. Mol. Biol.,* **22**, 192-8.

De March, M., Merino, N., Barrera-Vilarmau, S., Crehuet, R., Onesti, S., Blanco, F. J., De Biasio, A. (2017) Structural basis of human PCNA sliding on DNA. *Nat. Commun.,* **8**, 13935.

Deegan, T. D., Yeeles, J. T. and Diffley, J. F. (2016) Phosphopeptide binding by Sld3 links Dbf4-dependent kinase to MCM replicative helicase activation. *EMBO J.*, **35**, 961-73.

Deshpande, A. M., Ivanova, I. G., Raykov, V., Xue, Y. and Maringele, L. (2011) Polymerase epsilon is required to maintain replicative senescence. *Mol. Cell. Biol.*, **31**, 1637-45.

Devbhandari, S., Jiang, J., Kumar, C., Whitehouse, I. and Remus, D. (2017) Chromatin Constrains the Initiation and Elongation of DNA Replication. *Mol. Cell*, **65**, 131-41.

Dewar, J. M., Low, E., Mann, M., Räschle, M. and Walter, J. C. (2017) CRL2(Lrr1) promotes unloading of the vertebrate replisome from chromatin during replication termination. *Genes Dev.*, **31**, 275-90.

Diffley, J. F. and Cocker, J. H. (1992) Protein-DNA interactions at a yeast replication origin. *Nature*, **357**, 169-72.

Dmowski, M., Rudzka, J., Campbell, J. L., Jonczyk, P. and Fijałkowska, I. J. (2017) Mutations in the Non-Catalytic Subunit Dpb2 of DNA Polymerase Epsilon Affect the Nrm1 Branch of the DNA Replication Checkpoint. *PLoS Genet.,* **13**, e1006572.

Ellison, V. and Stillman, B. (2003) Biochemical characterization of DNA damage checkpoint complexes: clamp loader and clamp complexes with specificity for 5′ recessed DNA. *PLoS Biol.,* **1**, 231-43.

Evrin, C., Clarke, P., Zech, J., Lurz, R., Sun, J., Uhle, S., Li, H., Stillman, B. and Speck, C. (2009) A double-hexameric MCM2-7 complex is loaded onto origin DNA during licensing of eukaryotic DNA replication. *Proc. Natl. Acad. Sci. USA.,* **106**, 20240-5.

Fanning, E., Klimovich, V., and Nager, A. R. (2006) A dynamic model for replication protein A (RPA) function in DNA processing pathways. *Nucleic Acids Res.,* **34**, 4126-37.

Feng, W. and D'Urso, G. (2001). Schizosaccharomyces pombe cells lacking the amino-terminal catalytic domains of DNA polymerase epsilon are viable but require the DNA damage checkpoint control. Mol. Cell. Biol., **21**, 4495-504.

Foltman, M., Evrin, C., De Piccoli, G., Jones, R. C., Edmondson, R. D., Katou, Y., Nakato, R., Shirahige, K. and Labib, K. (2013) Eukaryotic replisome components cooperate to process histones during chromosome replication. *Cell Rep.,* **3**, 892-904.

Fu, Y. V., Yardimci, H., Long, D. T., Ho, T. V., Guainazzi, A., Bermudez, V. P., Hurwitz, J., van Oijen, A., Schärer, O. D. and Walter, J. C. (2011) Selective Bypass of a Lagging Strand Roadblock by the Eukaryotic Replicative DNA Helicase. *Cell,* **146**, 931-41.

Fukuda, K., Morioka, H., Imajou, S., Ikeda, S., Ohtsuka, E. and Tsurimoto, T. (1995) Structure-function relationship of the eukaryotic DNA replication factor, proliferating cell nuclear antigen. *J. Biol. Chem.*, **270**, 22527-34.

Gaillard, H., García-Muse, T. and Aguilera, A. (2015) Replication stress and cancer. *Nat. Rev. Cancer,* **15**, 276-89.

Gambus, A., van Deursen, F., Polychronopoulos, D., Foltman, M., Jones, R. C., Edmondson, R. D., Calzada, A. and Labib, K. (2009) A key role for Ctf4 in coupling the MCM2-7 helicase to DNA polymerase alpha within the eukaryotic replisome. *EMBO J.*, **28**, 2992-3004.

Gao, H., Moss, D. L., Parke, C., Tatum, D. and Lustig, A. J. (2014) The Ctf18RFC clamp loader is essential for telomere stability in telomerase-negative and mre11 mutant alleles. *PLoS One,* **9,** e88633.

Gavin, A. C., Bösche, M., Krause, R., Grandi, P., Marzioch, M., Bauer, A., Schultz, J., Rick, J. M., Michon, A. M., Cruciat, C. M., Remor, M., Höfert, C., Schelder, M., Brajenovic, M., Ruffner, H., Merino, A., Klein, K., Hudak, M., Dickson, D., Rudi, T., Gnau, V., Bauch, A., Bastuck, S., Huhse, B., Leutwein, C., Heurtier, M. A., Copley, R. R., Edelmann, A., Querfurth, E., Rybin, V., Drewes, G., Raida, M., Bouwmeester, T., Bork, P., Seraphin, B., Kuster, B., Neubauer, G. and Superti-Furga, G. (2002) Functional organization of the yeast proteome by systematic analysis of protein complexes. *Nature*, **415**, 141-7.

García-Rodríguez, L. J., De Piccoli, G., Marchesi, V., Jones, R. C., Edmondson, R. D. and Labib, K. (2015) A conserved Polε binding module in Ctf18-RFC is required for S-phase checkpoint activation downstream of Mec1. *Nucleic Acids Res.,* **18**, 8830-8.

Gellon, L., Razidlo, D. F., Gleeson, O., Verra, L., Schulz, D., Lahue, R. S. and Freudenreich, C. H. (2011) New functions of Ctf18-RFC in preserving genome stability outside its role in sister chromatid cohesion. *PLoS Genet.*, **7**, e1001298.

Georgescu, R. E, Langston, L., Yao, N. Y., Yurieva, O., Zhang, D., Finkelstein, J., Agarwal, T., and O'Donnell, M. E. (2014) Mechanism of asymmetric polymerase assembly at the eukaryotic replication fork. *Nat. Struct. Mol. Biol.,* **21**, 664-70.

Georgescu, R. E., Schauer, G. D., Yao, N. Y., Langston, L. D., Yurieva, O., Zhang, D.,

Finkelstein, J. and O'Donnell, M. E. (2015a) Reconstitution of a eukaryotic replisome reveals suppression mechanisms that define leading/lagging strand operation. *eLife,* **4**, e04988.

Georgescu, R. E., Langston, L. D. and O'Donnell, M. E. (2015b) A proposal: Evolution of PCNA's role as a marker of newly replicated DNA. *DNA Repair (Amst)*, **29**, 4-15.

Giannattasio, M. and Branzei, D. (2017) S-phase checkpoint regulations that preserve replication and chromosome integrity upon dNTP depletion. *Cell Mol. Life Sci.,* **74**, 2361-80.

Gomes, X. V. and Burgers, P. M. (2001) ATP utilization by yeast replication factor C. I. ATP-mediated interaction with DNA and with proliferating cell nuclear antigen. *J. Biol. Chem.*, **276**, 34768-75.

Grabarczyk, D. B., Silkenat, S. and Kisker, C. (2018) Structural Basis for the Recruitment of Ctf18-RFC to the Replisome. *Structure*, **26**, 137-44.

Graham, J. E., Marians, K. J. and Kowalczykowski, S. C. (2017) Independent and Stochastic Action of DNA Polymerases in the Replisome. *Cell*, **169**, 1201-13.

Handa, T., Kanke, M., Takahashi, T. S., Nakagawa, T. and Masukata, H. (2012) DNA polymerization-independent functions of DNA polymerase epsilon in assembly and progression of the replisome in fission yeast. *Mol. Biol. Cell*, **23**, 3240-53.

Hanna, J. S., Kroll, E. S., Lundblad, V. and Spencer, F. A. (2001) Saccharomyces cerevisiae CTF18 and CTF4 are required for sister chromatid cohesion. *Mol. Cell. Biol.,* **21**, 3144-58.

Hedglin, M., Kumar, R. and Benkovic, S. J. (2013) Replication clamps and clamp loaders. *Cold Spring Harb. Perspect. Biol.,* **5**, a010165.

Heller, R. C., Kang, S., Lam, W. M., Chen, S., Chan, C. S. and Bell, S. P. (2011) Eukaryotic origin-dependent DNA replication in vitro reveals sequential action of DDK and S-CDK kinases. *Cell*, **146**, 80-91.

Henninger, E. E. and Pursell, Z. F. (2014) DNA polymerase ε and its roles in genome stability. *IUBMB life,* **66**, 339-51.

Henricksen, L. A., Umbricht, C. B. and Wold, M. S. (1994) Recombinant replication protein A: expression, complex formation, and functional characterization. *J. Biol. Chem.*, **269**, 11121-32.

Higashi, T. L., Ikeda, M., Tanaka, H., Nakagawa, T., Bando, M., Shirahige, K., Kubota, Y., Takisawa, H., Masukata, H. and Takahashi, T. S. (2012) The prereplication complex recruits XEco2 to chromatin to promote cohesin acetylation in Xenopus egg extracts. *Curr. Biol.,* **22**, 977-88.

Hingorani, M. M. and Coman, M. M. (2002) On the specificity of interaction between the Saccharomyces cerevisiae clamp loader replication factor C and primed DNA templates during DNA replication. *J. Biol. Chem.*, **277**, 47213-24.

Hiraga, S., Robertson, E. D. and Donaldson, A. D. (2006) The Ctf18 RFC−like complex positions yeast telomeres but does not specify their replication time. *EMBO J.,* **25**, 1505-14.

Hogg, M., Osterman, P., Bylund, G. O., Ganai, R. A., Lundström, E. B., Sauer-Eriksson, A. E. and Johansson, E. (2014) Structural basis for processive DNA synthesis by yeast DNA polymerase ε. *Nat. Struct. Mol. Biol.,* **21**, 49-55.

Hou, F. and Zou, H. (2005) Two human orthologues of Eco1/Ctf7 acetyltransferases are both required for proper sister-chromatid cohesion. *Mol. Biol. Cell,* **16**, 3908-18.

Iida, T. and Araki, H. (2004) Noncompetitive counteractions of DNA polymerase epsilon and ISW2/yCHRAC for epigenetic inheritance of telomere position effect in Saccharomyces cerevisiae. *Mol. Cell. Biol.,* **24**, 217-27.

Johansson, E. and Dixon, N. (2013) Replicative DNA polymerases. *Cold Spring Harb. Perspect. Biol.,* **5**, a012799.

Johnson, R. E., Klassen, R., Prakash, L. and Prakash, S. (2015) A Major Role of DNA Polymerase δ in Replication of Both the Leading and Lagging DNA Strands. *Mol. Cell,* **59**, 163-75.

Kamimura, Y., Tak, Y. S., Sugino, A. and Araki, H. (2001) Sld3, which interacts with Cdc45 (Sld4), functions for chromosomal DNA replication in Saccharomyces cerevisiae. *EMBO J.*, **20**, 2097-107.

Kanellis, P., Agyei, R. and Durocher, D. (2003) Elg1 Forms an Alternative PCNA-Interacting RFC complex required to maintain genome stability. *Curr. Biol., **13***, 1583-95.

Kang, Y. H., Galal, W. C., Farina, A., Tappin, I. and Hurwitz, J. (2012) Properties of the human Cdc45/Mcm2-7/GINS helicase complex and its action with DNA polymerase epsilon in rolling circle DNA synthesis. *Proc. Natl. Acad. Sci. USA.,* **109**, 6042-7.

Kanke, M., Tahara, E., Huis In't Veld, P. J. and Nishiyama, T. (2016) Cohesin acetylation and Wapl-Pds5 oppositely regulate translocation of cohesin along DNA. *EMBO J.,* **35**, 2686-98.

Kelch, B. A. (2016) Review: The lord of the rings: Structure and mechanism of the sliding clamp loader. *Biopolymers,* **105**, 532-46.

Kesti, T., Flick, K., Keränen, S., Syväoja, J. E. and Wittenberg, C. (1999) DNA polymerase epsilon catalytic domains are dispensable for DNA replication, DNA repair, and cell viability. *Mol. Cell*, **3**, 679-85.

Khair, L., Chang, Y. T., Subramanian, L., Russell, P. and Nakamura, T. M. (2010) Roles of the checkpoint sensor clamp Rad9-Rad1-Hus1 (911)-complex and the clamp loaders Rad17-RFC and Ctf18-RFC in Schizosaccharomyces pombe telomere maintenance. *Cell Cycle*, **9**, 2237-48.

Kouprina, N., Tsouladze, A., Koryabin, M., Hieter, P., Spencer, F. and Larionov, V. (1993) Identification and genetic mapping of CHL genes controlling mitotic chromosome transmission in yeast. *Yeast*, **9**, 11-9.

Krishna, T. S., Kong, X. P., Gary, S., Burgers, P. M. and Kuriyan, J. (1994) Crystal structure of the eukaryotic DNA polymerase processivity factor PCNA. *Cell*, **79**, 1233-43.

Kubota, T., Hiraga, S., Yamada, K., Lamond, A. I. and Donaldson, A. D. (2011) Quantitative proteomic analysis of chromatin reveals that Ctf18 acts in the DNA replication checkpoint. *Mol. Cell. Proteomics,* **10**, M110.005561.

Kubota, T., Nishimura, K., Kanemaki, M. T. and Donaldson, A D. (2013a) The Elg1 replication factor C-like complex functions in PCNA unloading during DNA replication. *Mol. Cell,* **50**, 273-80.

Kubota, T., Myung, K. and Donaldson, A. D. (2013b) Is PCNA unloading the central function of the Elg1/ATAD5 replication factor C-like complex? *Cell Cycle*, **12**, 2570-9.

Kunkel, T.A., Sabatino, R.D. and Bambara, R.A. (1987) Exonucleolytic proofreading by calf thymus DNA polymerase delta. *Proc. Natl. Acad. Sci. USA.,* **84**, 4865-9.

Lagrange, T., Kim, T. K., Orphanides, G., Ebright, Y. W., Ebright, R. H. and Reinberg, D. (1996) High-resolution mapping of nucleoprotein complexes by site-specific protein-DNA photocrosslinking: organization of the human TBP-TFIIA-TFIIB-DNA quaternary complex. *Proc. Natl. Acad. Sci. USA.,* **93**, 10620-5.

Le, H. P., Masuda, Y., Tsurimoto, T., Maki, S., Katayama, T., Furukohri, A. and Maki, H. (2015) Short CCG repeat in huntingtin gene is an obstacle for replicative DNA polymerases, potentially hampering progression of replication fork. *Genes Cells,* **20**, 817-833.

Lee, D. G. and Bell, S. P. (1997) Architecture of the yeast origin recognition complex bound to origins of DNA replication. *Mol. Cell. Biol.,* **17**, 7159-68.

Lengronne, A., McIntyre, J., Katou, Y., Kanoh, Y., Hopfner, K. P., Shirahige, K. and Uhlmann, F. (2006) Establishment of sister chromatid cohesion at the S. cerevisiae replication fork. *Mol. Cell,* **23**, 787-99.

Leonard, A. C. and Méchali, M. (2013) DNA replication origins. *Cold Spring Harb. Perspect. Biol.*, **5**, a010116.

Li, Y., Asahara, H., Patel, V. S., Zhou, S. and Linn, S. (1997) Purification, cDNA cloning, and gene mapping of the small subunit of human DNA polymerase epsilon. *J. Biol. Chem.,* **272**, 32337-44.

Li, F., Martienssen, R. and Cande, W. Z. (2011) Coordination of DNA replication and histone modification by the Rik1-Dos2 complex. *Nature*, **475**, 244-8.

Li, H. and Stillman, B. (2012) The origin recognition complex: a biochemical and structural view. *Subcell. Biochem.*, **62**, 37-58.

Lopes, J., Piazza, A., Bermejo, R., Kriegsman, B., Colosio, A., Teulade-Fichou, M. P., Foiani, M. and Nicolas, A. (2011) G-quadruplex-induced instability during leading-strand replication. *EMBO J.*, **30**, 4033-46.

Lopez, B. S., Pasero, P. and Lambert, S. A. (2014) The causes of replication stress and their consequences on genome stability and cell fate. *Semin. Cell Dev. Biol.,* **30**, 154-64.

Lõoke, M., Maloney, M.F. and Bell, S.P. (2017) Mcm10 regulates DNA replication elongation by stimulating the CMG replicative helicase. *Genes Dev.*, **31**, 291-305.

Losada, A., Hirano, M. and Hirano, T. (1998) Identification of Xenopus SMC protein complexes required for sister chromatid cohesion. *Genes Dev.*, **12**, 1986-97.

Lou, H., Komata, M., Katou, Y., Guan, Z., Reis, C. C., Budd, M., Shirahige, K. and Campbell, J. L. (2008) Mrc1 and DNA polymerase epsilon function together in linking DNA replication and the S phase checkpoint. *Mol. Cell*, **32**, 106-17.

Maradeo, M. E. and Skibbens, R. V. (2009) The Elg1-RFC clamp-loading complex performs a role in sister chromatid cohesion. *PLoS One,* **4**, e4707.

Marzahn, M. R., Hayner, J. N., Meyer, J.A. and Bloom, L. B. (2015) Kinetic analysis of PCNA clamp binding and release in the clamp loading reaction catalyzed by Saccharomyces cerevisiae replication factor C. *Biochim. Biophys. Acta.,* **1854**, 31-8.

Masuda, Y., Suzuki, M., Piao, J., Gu, Y., Tsurimoto, T. and Kamiya K. (2007) Dynamics of human replication factors in the elongation phase of DNA replication. *Nucleic Acids Res.*, **35**, 6904-16.

Mayer, M. L., Gygi, S. P., Aebersold, R. and Hieter, P. (2001) Identification of RFC (Ctf18p, Ctf8p, Dcc1p): An alternative RFC complex required for sister chromatid cohesion in S. cerevisiae. *Mol. Cell,* **7**, 959-70.

Mclnerney, P., Johnson, A., Katz, F. and O'Donnell, M. (2007) Characterization of a triple DNA polymerase replisome. *Mol. Cell*, **27**, 527-38.

Merkle, C. J., Karnitz, L. M., Henry-Sánchez, J. T. and Chen, J. (2003) Cloning and characterization of hCTF18, hCTF8, and hDCC1. Human homologs of a Saccharomyces cerevisiae complex involved in sister chromatid cohesion establishment. *J. Biol. Chem.,* **278**, 30051-6.

Michaelis, C., Ciosk, R. and Nasmyth, K. (1997) Cohesins: chromosomal proteins that prevent premature separation of sister chromatids. *Cell*, **91**, 35-45.

Miyabe, I., Mizuno, K., Keszthelyi, A., Daigaku, Y., Skouteri, M., Mohebi, S., Kunkel, T. A., Murray, J. M. and Carr, A. M. (2015) Polymerase δ replicates both strands after homologous recombination-dependent fork restart. *Nat. Struct. Mol. Biol.*, **22**, 932-8.

Moldovan, G. L., Pfander, B. and Jentsch, S. (2006) PCNA controls establishment of sister chromatid cohesion during S phase. *Mol. Cell*, **23**, 723-32.

Moldovan, G. L., Pfander, B. and Jentsch, S. (2007) PCNA, the maestro of the replication fork. *Cell,* **129**, 665-79.

Morrison, A., Araki, H., Clark, A. B., Hamatake, R. K. and Sugino, A. (1990) A third essential DNA polymerase in *S. cerevisiae. Cell*, **62**, 1143-51.

Morrison, A., Bell, J. B., Kunkel, T. A. and Sugino, A. (1991) Eukaryotic DNA polymerase amino acid sequence required for 3'----5' exonuclease activity. *Proc. Natl. Acad. Sci. USA.,* **88**, 9473-7.

Moser, J., Kool, H., Giakzidis, I., Caldecott, K., Mullenders, L. H. and Fousteri, M. I. (2007) Sealing of chromosomal DNA nicks during nucleotide excision repair requires XRCC1 and DNA ligase III alpha in a cell-cycle-specific manner. *Mol. Cell,* **27**, 311-23.

Murakami, T., Takano, R., Takeo, S., Taniguchi, R., Ogawa, K., Ohashi, E. and Tsurimoto, T. (2010) Stable interaction between the human proliferating cell nuclear antigen loader complex Ctf18-replication factor C (RFC) and DNA polymerase ε is mediated by the cohesion-specific subunits, Ctf18, Dcc1, and Ctf8. *J. Biol. Chem.,* **285**, 34608-15.

Muramatsu, S., Hirai, K., Tak, Y. S., Kamimura, Y. and Araki, H. (2010) CDK-dependent complex formation between replication proteins Dpb11, Sld2, Pol (epsilon), and GINS in budding yeast. *Genes Dev*., **24**, 602-12.

Naiki, T., Kondo, T., Nakada, D., Matsumoto, K. and Sugimoto, K. (2001) Chl12 (Ctf18) forms a novel replication factor C-related complex and functions redundantly with Rad24 in the DNA replication checkpoint pathway. *Mol. Cell. Biol.,* **21**, 5838-45.

Narita, T., Tsurimoto, T., Yamamoto, J., Nishihara, K., Ogawa, K., Ohashi, E., Evans, T., Iwai, S., Takeda, S. and Hirota, K. (2010) Human replicative DNA polymerase δ can bypass T-T (6-4) ultraviolet photoproducts on template strands. *Genes Cells,* **15**, 1228-3.

Navadgi-Patil, M. V. and Burgers, M. P. (2009) A tale of two tails: Activation of DNA damage checkpoint kinase Mec1/ATR by the 9-1-1 clamp and by Dpb11/TopBP1. *DNA Repair,* **8**, 996-1003.

Navas, T. A., Zhou, Z. and Elledge, S. J. (1995) DNA polymerase epsilon links the DNA replication machinery to the S phase checkpoint. *Cell*, **80**, 29-39.

Navas, T. A., Sanchez, Y. and Elledge, S. J. (1996) RAD9 and DNA polymerase epsilon form parallel sensory branches for transducing the DNA damage checkpoint signal in Saccharomyces cerevisiae. *Genes Dev.*, **10**, 2632-43.

Nick McElhinny, S. A., Gordenin, D. A., Stith, C. M., Burgers, P. M. and Kunkel, T. A. (2008) Division of labor at the eukaryotic replication fork. *Mol. Cell*, **30**, 137-44.

Ogi, T., Limsirichaikul, S., Overmeer, R. M., Volker, M., Takenaka, K., Cloney, R., Nakazawa, Y., Niimi, A., Miki, Y., Jaspers, N. G., Mullenders, L. H., Yamashita, S., Fousteri, M. I. and Lehmann, A. R. (2010) Three DNA polymerases, recruited by different mechanisms, carry out NER repair synthesis in human cells. *Mol. Cell*, **37**, 714-27.

Ogiwara, H., Ohuchi, T., Ui, A., Tada, S., Enomoto, T. and Seki, M. (2007) Ctf18 is required for homologous recombination-mediated double-strand break repair. *Nucleic Acids Res.,* **35**, 4989-5000.

Ohya, T., Maki, S., Kawasaki, Y. and Sugino, A. (2000) Structure and function of the fourth subunit (Dpb4p) of DNA polymerase epsilon in Saccharomyces cerevisiae. *Nucleic Acids Res.*, **28**, 3846-52.

Okimoto, H., Tanaka, S., Araki, H., Ohashi, E. and Tsurimoto, T. (2016) Conserved interaction of Ctf18-RFC with DNA polymerase ε is critical for maintenance of genome stability in Saccharomyces cerevisiae. *Genes Cells,* **21**, 482-91.

Parnas, O., Zipin-Roitman, A., Mazor, Y., Liefshitz, B., Ben-Aroya, S. and Kupiec, M. (2009) The ELG1 clamp loader plays a role in sister chromatid cohesion. *PLoS One,* **4**, e5497.

Pellegrini, L. (2012) The Pol α-primase complex. *Subcell. Biochem.*, **62**, 157-69.

Peters, J. M. and Nishiyama, T. (2012) Sister chromatid cohesion. *Cold Spring Harb. Perspect. Biol.,* **4**, a011130.

Puddu, F., Piergiovanni, G., Plevani, P. and Muzi-Falconi, M. (2011) Sensing of replication stress and Mec1 activation act through two independent pathways involving the 9-1-1 complex and DNA polymerase ε. *PLoS Genet.,* **7**, e1002022.

Pursell, Z. F., Isoz, I., Lundström, E. B., Johansson, E., and Kunkel, T. A. (2007) Yeast DNA Polymerase ε Participates in Leading-Strand DNA Replication. *Science*, **317**, 127-30.

Remus, D., Beuron, F., Tolun, G., Griffith, J. D., Morris, E. P. and Diffley, J. F. (2009) Concerted loading of Mcm2-7 double hexamers around DNA during DNA replication origin licensing. *Cell*, **139**, 719-30.

Riera, A., Tognetti, S. and Speck, C. (2014) Helicase loading: how to build a MCM2-7 double-hexamer. *Semin. Cell Dev. Biol.*, **30**, 104-9.

Riera, A., Barbon, M., Noguchi, Y., Reuter, L.M., Schneider, S. and Speck, C. (2017) From structure to mechanism-understanding initiation of DNA replication. *Genes Dev.,* **31**, 1073-88.

Rolef Ben-Shahar, T., Heeger, S., Lehane, C., East, P., Flynn, H., Skehel, M. and Uhlmann, F. (2008) Eco1-dependent cohesin acetylation during establishment of sister chromatid cohesion. *Science*, **321**, 563-6.

Saka, K., Takahashi, A., Sasaki, M. and Kobayashi, T. (2016) More than 10% of yeast genes are related to genome stability and influence cellular senescence via rDNA maintenance. *Nucleic Acids Res.,* **44**, 4211-21.

Sakato, M., Zhou, Y. and Hingorani, M. M. (2012) ATP binding and hydrolysis-driven rate-determining events in the RFC-catalyzed PCNA clamp loading reaction. *J. Mol. Biol.,* **416**, 176-91.

Saldivar, J. C., Cortez, D. and Cimprich, K. A. (2017) The essential kinase ATR: ensuring faithful duplication of a challenging genome. *Nat. Rev. Mol. Cell Biol.,* **18**, 622-36.

Sengupta, S., van Deursen, F., De Piccoli, G. and Labib, K. (2013) Dpb2 integrates the leading-strand DNA polymerase into the eukaryotic replisome. *Curr. Biol.*, **23**, 543-52.

Shiomi, Y., Usukura, J., Masamura, Y., Takeyasu, K., Nakayama, Y., Obuse, C., Yoshikawa, H. and Tsurimoto, T. (2000) ATP-dependent structural change of the eukaryotic clamp-loader protein, replication factor C. *Proc. Natl. Acad. Sci. USA.,* **97**, 14127-32.

Shiomi, Y., Shinozaki, A., Sugimoto, K., Usukura, J., Obuse, C. and Tsurimoto, T. (2004) The reconstituted human Chl12-RFC complex functions as a second PCNA loader. *Genes Cells,* ***9***, 279-90.

Shiomi, Y., Masutani, C., Hanaoka, F., Kimura, H. and Tsurimoto, T. (2007) A second proliferating cell nuclear antigen loader complex, Ctf18-Raplication Factor C, stimulates DNA polymerase η activity. *J. Biol. Chem.*, **282**, 20906-14.

Shiomi, Y., Hayashi, A., Ishii, T., Shinmyozu, K., Nakayama, J., Sugasawa, K. and Nishitani, H. (2012) Two different replication factor C proteins, Ctf18 and RFC1, separately control PCNA-CRL4Cdt2-mediated Cdt1 proteolysis during S phase and following UV irradiation. *Mol. Cell. Biol.,* **32**, 2279-88.

Shiomi, Y. and Nishitani, H. (2013) Alternative replication factor C protein, Elg1, maintains chromosome stability by regulating PCNA levels on chromatin. *Genes Cells,* **18**, 946-59.

Sirbu, B. M., McDonald, W. H., Dungrawala, H., Badu-Nkansah, A., Kavanaugh, G. M., Chen, Y., Tabb, D. L. and Cortez, D. (2013) Identification of proteins at active, stalled, and collapsed replication forks using isolation of proteins on nascent DNA (iPOND) coupled with mass spectrometry. *J. Biol. Chem.,* **288**, 31458-67.

Skibbens, R. V., Corson, L. B., Koshland, D. and Hieter, P. (1999) Ctf7p is essential for sister chromatid cohesion and links mitotic chromosome structure to the DNA replication machinery. *Genes Dev.*, **13**: 307-19.

Smith, D. J. and Whitehouse, I. (2012) Intrinsic coupling of lagging-strand synthesis to chromatin assembly. *Nature*, **483**, 434-8.

Song, J., Lafont, A., Chen, J., Wu, F. M., Shirahige, K. and Rankin, S. (2012) Cohesin acetylation promotes sister chromatid cohesion only in association with the replication machinery. *J. Biol. Chem.*, **287**, 34325-36.

Sonneville, R., Moreno, S. P., Knebel, A., Johnson, C., Hastie, C. J., Gartner, A., Gambus, A. and Labib, K. (2017) CUL-2(LRR-1) and UBXN-3 drive replisome disassembly during DNA replication termination and mitosis. *Nat. Cell Biol.,* **19**, 468-79.

Spencer, F., Gerring, S. L., Connelly, C. and Hieter, P. (1990) Mitotic chromosome transmission fidelity mutants in Saccharomyces cerevisiae. *Genetics*, **124**, 237-49.

Stith, C. M., Sterling, J., Resnick, M. A., Gordenin, D. A. and Burgers, P. M. (2008) Flexibility of eukaryotic Okazaki fragment maturation through regulated strand displacement synthesis. *J. Biol. Chem.*, **283**, 34129-40.

Sun, J., Shi, Y., Georgescu, R. E., Yuan, Z., Chait, B. T., Li, H. and O'Donnell, M. E. (2015) The architecture of a eukaryotic replisome. *Nat. Struct. Mol. Biol.,* **22**, 976-82.

Sun, Q., Tsurimoto, T., Juillard, F., Li, L., Li, S., De León Vázquez, E., Chen, S. and Kaye, K. (2014) Kaposi's sarcoma-associated herpesvirus LANA recruits the DNA polymerase clamp loader to mediate efficient replication and virus persistence. *Proc. Natl. Acad. Sci. USA.,* **111**, 11816-21.

Sutani, T., Kawaguchi, T., Kanno, R., Itoh, T. and Shirahige, K. (2009) Budding yeast Wpl1(Rad61)-Pds5 complex counteracts sister chromatid cohesion-establishing reaction. *Curr. Biol.,* **19**, 492-7.

Tahirov, T. H., Makarova, K. S., Rogozin, I. B., Pavlov, Y. I. and Koonin, E. V. (2009) Evolution of DNA polymerases: an inactivated polymerase-exonuclease module in Pol epsilon and a chimeric origin of eukaryotic polymerases from two classes of archaeal ancestors. *Biol. Direct.,* **4**, 11.

Takahashi, N., Quimbaya, M., Schubert, V., Lammens, T., Vandepoele, K., Schubert, I., Matsui, M., Inzé, D., Berx, G. and De Veylder, L. (2010) The MCM-binding protein ETG1 aids sister chromatid cohesion required for postreplicative homologous recombination repair. *PLoS Genet.*, **6**, e1000817.

Takahashi, T. S., Yiu, P., Chou, M. F., Gygi, S. and Walter, J. C. (2004) Recruitment of Xenopus Scc2 and cohesin to chromatin requires the pre-replication complex. *Nat. Cell. Biol.*, **6**, 991-6.

Tanaka, H., Katou, Y., Yagura, M., Saitoh, K., Itoh, T., Araki, H., Bando, M. and Shirahige, K. (2009) Ctf4 coordinates the progression of helicase and DNA polymerase alpha. *Genes Cells*, **14**, 807-20.

Tanaka, S., Umemori, T., Hirai, K., Muramatsu, S., Kamimura, Y. and Araki, H. (2007) CDK-dependent phosphorylation of Sld2 and Sld3 initiates DNA replication in budding yeast. *Nature*, **445**, 328-32.

Terret, M. E., Sherwood, R., Rahman, S., Qin, J. and Jallepalli, P. V. (2009) Cohesin acetylation speeds the replication fork. *Nature,* **462**, 231-5.

Tomasetti, C. and Vogelstein, B. (2015) Cancer etiology. Variation in cancer risk among tissues can be explained by the number of stem cell divisions. *Science*, **347**, 78-81.

Tong, K. and Skibbens, R. V. (2015) Pds5 regulators segregate cohesion and condensation pathways in Saccharomyces cerevisiae. *Proc. Natl. Acad. Sci. USA.,* **112**, 7021-6.

Truong, L. N. and Wu, X. (2011) Prevention of DNA re-replication in eukaryotic cells. *J. Mol. Cell. Biol.,* **3**, 13-22.

Tsubota, T., Tajima, R., Ode, K., Kubota, H., Fukuhara, N., Kawabata, T., Maki, S. and Maki, H. (2006) Double-stranded DNA binding, an unusual property of DNA polymerase epsilon, promotes epigenetic silencing in Saccharomyces cerevisiae. *J. Biol. Chem.,* **281**, 32898-908.

Tsurimoto, T., Melendy, T., and Stillman, B. (1990) Sequential initiation of lagging and leading strand synthesis by two different polymerase complexes at the SV40 DNA replication origin. *Nature*, **346**, 534-9.

Tsurimoto, T. and Stillman, B. (1991) Replication factors required for SV40 DNA replication in vitro. I. DNA structure-specific recognition of a primer-template junction by eukaryotic DNA polymerases and their accessory proteins. *J. Biol. Chem.,* **266**, 1950-60.

Uhlmann, F. and Nasmyth, K. (1998) Cohesion between sister chromatids must be established during DNA replication. *Curr. Biol.*, **8**, 1095-101.

Uhlmann, F. (2016) SMC complexes: from DNA to chromosomes. *Nat. Rev. Mol. Cell Biol.*, **17**, 399-412.

Vaisman, A. and Woodgate, R. (2017) Translesion DNA polymerases in eukaryotes: what makes them tick? *Crit. Rev. Biochem. Mol. Biol.,* **52**, 274-303.

Villa, F., Simon, A. C., Ortiz Bazan, M. A., Kilkenny, M. L., Wirthensohn, D., Wightman, M., Matak-Vinkovíc, D., Pellegrini, L. and Labib, K. (2016) Ctf4 Is a Hub in the Eukaryotic Replisome that Links Multiple CIP-Box Proteins to the CMG Helicase. *Mol. Cell*, **63**, 385-96.

Waga, S. and Stillman, B. (1998a) Cyclin-dependent kinase inhibitor p21 modulates the DNA primer-template recognition complex. *Mol. Cell. Biol.,* **18**, 4177-87.

Waga, S. and Stillman, B. (1998b) The DNA replication fork in eukaryotic cells. *Annu. Rev. Biochem.,* **67**, 721-51.

Weinert, T., Kaochar, S., Jones, H., Paek, A. and Clark, A. J. (2009) The replication fork's five degrees of freedom, their failure and genome rearrangements. *Curr. Opin. Cell Biol.*, **21**, 778-84.

Xu, H., Boone, C. and Brown, G. W. (2007) Genetic dissection of parallel sister-chromatid cohesion pathways. *Genetics*, **176**, 1417-29.

Yang, S. W. and Nash, H. A. (1994) Specific photocrosslinking of DNA-protein complexes: identification of contacts between integration host factor and its target DNA. *Proc. Natl. Acad. Sci. USA.,* **91**, 12183-7.

Yardimci, H., Loveland, A. B., Habuchi, S., van Oijen, A. M. and Walter, J. C. (2010) Uncoupling of sister replisomes during eukaryotic DNA replication. *Mol. Cell*, **40**, 834-40.

Yeeles, J. T., Deegan, T.D., Janska, A., Early, A. and Diffley, J.F. (2015) Regulated eukaryotic DNA replication origin firing with purified proteins. *Nature*, **519**, 431-5.

Yeeles, J. T., Janska, A., Early, A. and Diffley, J.F. (2017) How the Eukaryotic Replisome Achieves Rapid and Efficient DNA Replication. *Mol. Cell*, **65**, 105-16.

Yu, C., Gan, H., Han, J., Zhou, Z., Jia, S., Chabes, A., Farrugia, G., Ordog, T. and Zhang, Z. (2014) Strand-specific analysis shows protein binding at replication forks and PCNA unloading from lagging strands when forks stall. *Mol. Cell,* **56**, 551-63.

Zegerman, P. and Diffley, J. F. (2007) Phosphorylation of Sld2 and Sld3 by cyclin-dependent kinases promotes DNA replication in budding yeast. *Nature*, **445**, 281-5.

Zhang, J., Shi, X., Li, Y., Kim, B. J., Jia, J., Huang, Z., Yang, T., Fu, X., Jung, S. Y., Wang, Y., Zhang, P., Kim, S. T., Pan, X. and Qin, J. (2008) Acetylation of Smc3 by Eco1 is required for S phase sister chromatid cohesion in both human and yeast. *Mol. Cell,* **31**, 143-51.

Figure legend

Figure 1. Purified recombinant human proteins used in this study. About 0.5 μg proteins were separated by SDS-PAGE, and detected by CBB stain. Molecular masses of marker proteins (left) and analyzed proteins (right) were indicated.

Figure 2. PCNA loading by CTF18-RFC. (**A**) Schematic diagram of the PCNA loading assay with a gapped DNA attached to magnetic beads. A linearized 2.7 kb plasmid DNA harboring a 38 nt gap was used. After incubation of the DNA beads with purified proteins and ATP, the loaded PCNA was recovered from the DNA-beads bound fraction. (**B**) PCNA loading by 20–60 fmol of CTF18-RFC in the absence (lanes 2–5) or presence of 2 mM ATP (lanes 6–8) at 30 mM NaCl. Input control (12 fmol of trimeric PCNA) (lane 1) and 50% bound samples (lanes 2–8) were analyzed by immunoblotting with anti-PCNA antibody and quantified. 4.6, 14, 20 fmol of loaded PCNA corresponding to 0.5, 1.7 and 2.4 molecules of trimer PCNA per a 2.7 kb DNA were detected with 20, 40 and 60 fmol of CTF18-RFC (lanes 6–8).

Figure 3. PCNA loading by CTF18-RFC in the presence of Polε. 50% bound samples were analyzed by immunoblotting with anti-PCNA antibody (left), and the loaded PCNA was quantified and graphed with mean of two experimental replicates along with the individual values (right). (**A**) PCNA loading at 100 mM NaCl condition by 30-90 fmol of CTF18-RFC with either 100 fmol of Polε (lanes 6–9) or 100 fmol of Polδ (lanes 10–13), or without them (lanes 2–5). 12 fmol of PCNA was used as input control (lane 1). (**B**) PCNA loading by 15–45 fmol of CTF18-RFC with either 100 fmol of p261N (lanes 6–9) or 100 fmol of Polε (lanes 10–13), or without them (lanes 2–5). The 10 μl reaction mixture contained 30 mM NaCl, 40 mM creatine phosphate and 25 ng/μl creatine phosphate kinase. 17 fmol of PCNA was used as the input control (lane 1). (**C**) PCNA loading by 6–30 fmol of CTF18-RFC (top), 10–50 fmol of RFC (middle) or 10–50 fmol of CTF18-RFC(5) (bottom) in the same reaction mixture with 30 mM NaCl, 40 mM creatine phosphate, 25 ng/μl creatine phosphate kinase with or without 200 fmol of p261N. 17 fmol (top and middle) or 12 fmol (bottom) of PCNA was used as the input control (lane 1 of each).

Figure 4. Effects of salt concentrations and RPA on PCNA loading by CTF18-RFC. 12 fmol of PCNA (input control; lane 1), and 50% for (A) and (B) or whole for (C) of the bound samples were analyzed by immunoblotting with anti-PCNA antibody (left). The loaded PCNA was quantified and graphed with mean of two experimental replicates along with individual values (right). (**A**) Titration of NaCl concentration from 30 mM to 150 mM for PCNA loading by 50 fmol each of RFC (lanes 3–7) or CTF18-RFC (lanes 8–12). (**B**) Titration of NaCl (25–100 mM) for

PCNA loading by 30 fmol of CTF18-RFC with (lanes 7–11) or without (lanes 2–6) 200 fmol of p261N. (**C**) Effects of RPA (42, 85 fmol) on PCNA loading with 30 ng of gapped-DNA beads at 60 mM NaCl using 100 fmol of CTF18-RFC with (lanes 6–8) or without (lanes 3–5) 200 fmol of Polε. The whole bound fractions (lanes 2–8) and 42 fmol of RPA as the input control (lane 1) were detected by immunoblotting with anti-RPA serum (left, upper; RPA p70 subunit were indicated).

Figure 5. Analyses of bound CTF18-RFC and DNA polymerases on gapped DNA beads during PCNA loading. Pull-down assay with 30 ng of gapped DNA beads at 100 mM NaCl using 100 fmol of p261N (**A**), Polε (**B**), Polδ (**C**), 100 fmol of CTF18-RFC and 6.2 pmol of PCNA, as indicated. Input (10%; p261N, Polε, Polδ, CTF18-RFC) and 12 fmol of PCNA (lane 1), and 50% bound fractions (lanes 2–7), were analyzed by immunoblotting with the indicated antibodies (left). Bound % versus input of p261N/Polε and CTF18 from two experimental replicates were graphed with mean ± S.D. (right).

Figure 6. Properties of exonuclease deficient mutant of p261N. (**A**) Exonuclease assay of p261N (WT) and p261N^{exo-} (exo−). Reaction mixture (5 μl) containing 30 mM NaCl and 80 fmol of TEMP60 ssDNA labelled with ^{32}P at its 5′ end was incubated with 15–45 fmol of p261N (lanes 2–4) or p261N^{exo-} (lanes 5–7) at 37°C for 10 min. The reaction was stopped by addition of 10× loading solution (50% glycerol, 0.9% SDS, 0.05% bromophenol blue), and the products were separated by electrophoresis in 10% acrylamide gels in TAE and visualised by phosphor imaging. (**B**) PCNA loading with 10–30 fmol of CTF18-RFC and either 100 fmol of p261N (lanes 6–9) or 100 fmol of p261N^{exo-} (lanes 10–13), or without them (lanes 2–5), in 10 μl of reaction mixture containing 30 mM NaCl. Input of 12 fmol of PCNA (lane 1) and 50% bound samples (lanes 2–13) were analyzed by immunoblotting with anti-PCNA antibody. The loaded PCNA was quantified and graphed with mean of two distinct experimental replicates along with the individual values (bottom).

Figure 7. Analyses of PCNA loading on various structures of DNA. (**A**) Biotin-labeled 90-mer templates (BTN5 and BTN3) and primers for PCNA loading are indicated (see Table 1). These oligonucleotides are conjugated with streptavidin agarose ultra-performance beads. (**B**) PCNA loading with a 3′ and 5′ recessed primer-template DNA (3′/5′) beads. Reactions were performed at 30 mM NaCl with 6.2 pmol of PCNA and indicated combination of 4.2 pmol of RPA, 2 mM ATP, 50 fmol of CTF18-RFC. Input bands of 340 fmol of RPA, 12 fmol of PCNA (lane1), and 50% bound samples (lanes 2–9) are indicated. (**C**) PCNA loading with oligo-DNA beads containing

conjugated ssDNA (ss; BTN3), a 3′ and 5′ recessed primer-template DNA (3′/5′; BTN3 annealed with BTN30), a 3′ recessed primer-template DNA (3′; BTN3 annealed with BTN28), or a 5′ recessed primer-template DNA (5′; BTN5 annealed with BTN32). Reactions were performed at 120 mM NaCl with 6.2 pmol of PCNA, 4.2 pmol of RPA, 200 fmol of CTF18-RFC and the indicated combination of 2 mM ATP and 1 pmol of p261N^{exo-}. Input bands (lane 1) indicate 60 fmol (6%) of p261N^{exo-}, 10 fmol (5%) of CTF18-RFC, 340 fmol (8%) of RPA and 12 fmol of PCNA. Bound proteins were analyzed with 50% samples (lanes 2–13). Band intensities of PCNA were quantified and graphed with the mean ± S.D. from two experimental replicates (bottom). (**D**) The amounts of p261N^{exo-} and CTF18 that bound to four different DNA bead substrates were compared with or without ATP by quantification of their bound % versus input (100%) as indicated by the graph, with mean ± S.D. of two experimental replicates. (**E**) Pull-down assay of p261N^{exo-}. 27–80 fmol of p261N^{exo-} was incubated with magnetic beads conjugated with 250 fmol of an ssDNA (ss; BTN3), a dsDNA (ds; BTN3 annealed with TEMP90-R) or a 5′ and 3′ recessed primer-template DNA (3′/5′; BTN3 annealed with BTN30) in reaction mixture containing 100 mM NaCl at 32°C for 30 min. The reacted DNA beads were washed with 1× HBS three times, and p261N^{exo-} (40 fmol; lane 1) and 50% bound fractions (lanes 2–11) were detected by immunoblotting with anti-p261 antibody and graphed with mean of two experimental replicates along with the individual values (right). Lane 2 included magnetic beads only (−DNA).

Figure 8. Photo-crosslinking analyses of proteins directly bound to the primer strand of a primer-template junction. (**A**) A coupling scheme of APB with S-dNMP. By mixing of APB and an oligo DNA with a uniquely positioned phosphorothioate nucleotide (S-dNMP), the azidophenacyl group (AP) couples with the thiol group at the phosphodiester backbone. (**B**) The photo-crosslinking substrate DNA “AP-Junction” consisted of the labeled RF30 primer annealed with TEMP90-R. The azidophenacyl group (AP) was coupled with S-dCMP at the 3′ end of RF30 primer followed with two internal ^{32}P-TMP. The control DNA “AP-End” has AP at the blunted end by annealing of the labeled same primer with TEMP90-R neo. (**C**) Schematic diagram of photo-crosslinking assay. After incubation of a protein complex and a substrate DNA, UV was irradiated to crosslink the DNA with the protein subunit most proximal to the labeled site. Following nuclease treatment, the radiolabeled crosslinked proteins were detected by autoradiography after SDS-PAGE. (**D**) Photo-crosslinking of RFC (150 fmol) with 25 fmol AP-Junction (Junction; lanes 1–13) or AP-End (End; lanes 14–16) at 60 mM NaCl with (lanes 11–16) or without (lanes 1–10) 500 fmol of PCNA. A set of results without nucleotide (−) or with 2

mM ATP or 250 μM ATPγS (γS) is shown for each condition. Samples with (lanes 1–4, 8–16) or without (lanes 5–7) UV irradiation and with (lanes 8–16) or without (lanes 1–7) nuclease treatment were shown. Some background bands are indicated with an asterisk.

Figure 9. Photo-crosslinking analyses of the CTF18-RFC–p261N^{exo-} complex bound to 3′ primer at primer-template junction. (**A**) Photo-crosslinking of 150 fmol of CTF18-RFC with 25 fmol of AP-Junction at 60 mM (lanes 1–3) or 10 mM (lanes 4–9) NaCl in the presence (+) or absence (–) of 500 fmol of PCNA, as indicated. A set of results without nucleotides (−) or with 2 mM ATP or 250 μM ATPγS (γS) is shown for each condition. (**B**) The same photo-crosslinking of 150 fmol of CTF18-RFC, 250 fmol of CTF18-RFC(5) and 150 fmol of p261N^{exo-}, as indicated, in the presence of 500 fmol of PCNA and 250 μM ATPγS. (**C**) Crosslinked bands in (**B**) corresponding to p261N^{exo-} and CTF18 were quantified, and their relative intensities were graphed on the right using the highest intensity bands (lane 4) as reference (1.0), with mean ± S.D. of three experimental replicates. (**D**) The same photo-crosslinking of 150 fmol of p261N^{exo-}, 150 fmol of CTF18-RFC and 500 fmol of PCNA in the presence or absence of 2 mM ATP or 250 μM ATPγS. Crosslinked bands corresponding to p261N^{exo-} and CTF18 were quantified, and the relative values of CTF18/p261N^{exo-} are indicated below, with the ratio with ATPγS as 1.0.

Figure 10. Photo-crosslinking analyses of proteins directly bound to the template strand of a primer-template junction. (**A**) The template DNA, "AP-Template", had ^{32}P-TMP and S-dCMP at 25 nt and 26 nt from the 3′ end on a 90-mer oligonucleotide. (**B**) Three representatives of the primer-template junction substrates with differently positioned crosslinkers (azidophenacyl group; AP) relative to the 3′ primer end are indicated. In "–5", the AP is located in single-stranded DNA 5 nt away from the junction, in "±0" AP is at the junction and in "+10" AP is in double-stranded DNA 10 nt from the junction. (**C**) Photo-crosslinked bands from 25 fmol of indicated substrate DNA and 150 fmol of p261N^{exo-} (lanes 1–7, 15–21), or 150 fmol of CTF18-RFC (lanes 8–21) as indicated in the presence of 500 fmol of PCNA and 250 μM ATPγS. Protein bands corresponding to p261N^{exo-}, CTF18 and RFC2–5 are indicated. Relative band intensities of p261N^{exo-} and CTF18 using that of CTF18 in lane 16 as a reference (1.0) were measured and graphed on the right, with mean of three experimental replicates along with the individual values. (**D**) Photo-crosslinked bands from 25 fmol of indicated substrate DNAs with 2 mM ATP (lanes 1–7) or 250 μM ATPγS (lanes 8–14) in the presence of 150 fmol of p261N^{exo-}, 150 fmol of CTF18-RFC and 500 fmol of PCNA are shown, and quantified band intensities of p261N^{exo-} and CTF18 at each position were graphed (right), using CTF18 in lane 9 as a

reference (1.0), with mean of three experimental replicates along with the individual values.

Figure 11. Production of Polε in a DNA synthesizing mode using ddAMP at the 3′ primer end and incoming nucleotide. (**A**) Two 3′ primer-template junction substrates with ddAMP ("dd-Junction") or dAMP ("d-Junction") at their 3′ primer ends. (**B**) 60 fmol of Polε^{exo-} was mixed with 25 fmol of d-Junction ("d-J"; lanes 2, 3) or dd-Junction ("dd-J"; lanes 5, 6) at 60 mM NaCl in the presence (+) or absence (−) of 100 μM TTP in 5 μl volume, and binding was analyzed by EMSA after glutaraldehyde fixation. Lanes 1 and 4 were controls without Polε^{exo-}. Bands produced by binding of Polε^{exo-} to DNA are indicated. (**C**) Assembly of 60 fmol each of CTF18-RFC and Polε^{exo-} and 500 fmol of PCNA to 25 fmol of dd-Junction substrate was analyzed by EMSA as above (B) using indicated combinations of proteins at 60 mM NaCl. Additions of 100 μM TTP and 250 μM ATPγS are indicated by "+" and an asterisk (lane 3), respectively. DNA bands shifted at positions by added proteins are indicated at the right. (**D**) Assembly of 75 fmol each of CTF18-RFC or CTF18-RFC(5), 60 fmol of Polε^{exo-} and 500 fmol of PCNA to 25 fmol of dd-Junction substrate was analyzed by EMSA as above (B) using indicated combinations of proteins at 60 mM NaCl. DNA bands shifted at positions by added proteins are indicated at the right.

Figure 12. Analysis of PCNA loading in the presence of Polε in DNA synthesizing mode. (**A**) To study PCNA loading in the presence of Polε^{exo-} in DNA synthesizing mode, a gapped DNA with ddAMP at the 3′ primer end was prepared. The sequence shows a 51 bp region with the 35 nt gap on the substrate DNA. The nucleotides shown in bold represent sequence extension to prepare the 3′ primer end with ddAMP. (**B**) Comparison of PCNA loading with the gapped-DNA beads with Polε^{exo-} in non-synthesizing (–dGTP) and synthesizing (+dGTP) modes. The DNA beads (15 ng) were incubated with 100 fmol of CTF18-RFC and 6.2 pmol of PCNA in the presence of 0, 120, 240 and 360 fmol of Polε^{exo-} in a 10 μl reaction mixture at 60 mM NaCl. dGTP (100 μM) was added in lanes 7–11. Input control of 12 fmol of PCNA (lane 1) and 100% bound fractions (lanes 2–11) were applied to immunoblotting with anti-PCNA antibody. Lanes 2 and 7 were the negative controls without CTF18-RFC and Polε^{exo-}. Bound PCNA was quantified and graphed at the right with mean of two experimental replicates and those values.

Figure 13. Analyses of DNA synthesis by CTF18-RFC–Polε–PCNA. Product DNA profiles after electrophoresis in alkaline agarose gels are shown together with DNA size markers (right). (**A**) Holoenzyme assay was done with indicated combinations of 200 fmol of Polε, 600 fmol of CTF18-RFC, 2 pmol of PCNA and 6 pmol of RPA. Lower amounts of CTF18-RFC (400 or 200

fmol) were used in lanes 6 and 7. (**B**) Titration of Polε (+, ++, +++ for 147, 293, 440 fmol, respectively; lanes 2-8) or Polδ (+, ++, +++ for 53, 107, 160 fmol, respectively; lanes 9–15) in holoenzyme assay with 600 fmols of RFC (lanes 3–5, 10–12) or CTF18-RFC (lanes 6–8, 13–15) or without them (lanes 2 and 9) in the presence of 6 pmol of RPA and 2 pmol of PCNA.

Figure 14. A possible function of the CTF18-RFC–Polε complex in replication fork. (i) The leading-strand holoenzyme will consist of CMG helicase, Polε, CMG-associating factors (TIM/TIPIN and CLASPIN (Csm3/Tof1 and Mrc1 in *S. cerevisiae*)), and PCNA. I propose that CTF18-RFC is further involved in the complex through its interaction with Polε [(i) Synthesizing]. In this mode, the associated CTF18-RFC will have little opportunity to load fresh PCNA. By stochastic events or obstacles on the chromosome, Polε will uncouple from CMG helicase and PCNA [(ii) Stalling and Uncoupling from PCNA], and shifts in the DNA non-synthesizing mode. CTF18-RFC complexed with Polε will then be able to access the 3′ primer end and load fresh PCNA at the site [(iii) PCNA loading]. Then Polε associates with the fresh PCNA at the 3′ primer end and restart DNA synthesis [(iv) Synthesis restart], and continues the leading-strand synthesis [(i) Synthesizing]. Previous PCNA released from Polε will stay on the DNA and function as a scaffold for PCNA-binding proteins acting for post-replication processes.

Table 1 : Oligonucleotides DNAs

Name	Sequence (5′–3′)
BTN5	Biotin-tgaggttcagcaaggtgatgctttagatttttcatttgctgctggctctcagcgtggca-ctgttgcaggcggtgttaatactgaccgcct
BTN3	tgaggttcagcaaggtgatgctttagatttttcatttgctgctggctctcagcgtggcactgttgc-aggcggtgttaatactgaccgcct-Biotin
BTN32	aaaaatctaaagcatcaccttgctgaacctca
BTN30	cagtgccacgctgagagccagcagcaaatg
BTN28	aggcggtcagtattaacaccgcctgcaa
TEMP90-R	aggcggtcagtattaacaccgcctgcaacagtgccacgctgagagccagcagcaaatgaaaaatct-aaagcatcaccttgctgaacctca
TEMP90-R neo	gaaaaatctaaagcatcaccttgctgaacctcaaggcggtcagtattaacaccgcctgcaacagtg-ccacgctgagagccagcagcaaat
RF64	aggcggtcagtattaacaccgcctgcaacagtgccacgctgagagccagcagcaaatgaaaaat
TEMP60	tgaggttcagcaaggtgatgctttagatactgttgcaggcggtgttaatactgaccgcct
RF30	tgaggttcagcaaggtgatgctttagattt
RF46	tgaggttcagcaaggtgatgctttagattttcatttgctgctggc
RF41	tgaggttcagcaaggtgatgctttagattttcatttgctg
RF36	tgaggttcagcaaggtgatgctttagattttcatt
RF31	tgaggttcagcaaggtgatgctttagatttt
RF26	tgaggttcagcaaggtgatgctttag
RF21	tgaggttcagcaaggtgatgc
260NFw	ctagctagaaggaggccgg
260NEcoRV	ttaaccggcctccttctagctagccgg
HisSalIFw	tcgacatgcatcatcatcaccatcacc
HisSalIRv	tcgaggtgatggtgatgatgatgcatg

Acknowledgements

I would like to express my deepest appreciation to Prof. Toshiki Tsurimoto, who gave me the opportunity to study human CTF18-RFC and Polε biochemically. His constructive suggestions have always helped and encouraged me. I also appreciate Drs. Eiji Ohashi and Tatsuro S Takahashi for their comments and discussions, which was provided an enormous contribution to this work. I would also like to express my gratitude for Prof. Kouji Hirota for kind gift of p261^{exo-} vector as well as for constructive suggestions, for Dr. Hironori Kawakami for kind suggestions about photo-crosslinking experiment and providing S-dCTP.

I would also like to thank all the Tsurimoto lab members for helpful suggestions and for encouraging me. I am grateful to Ms. Eriko Sata in radioisotope research center in Kyushu University for continuous encouraging during my Ph.D. Finally, I owe my sincere appreciation to my family for their constant supports.

January 2018

Ryo Fujisawa

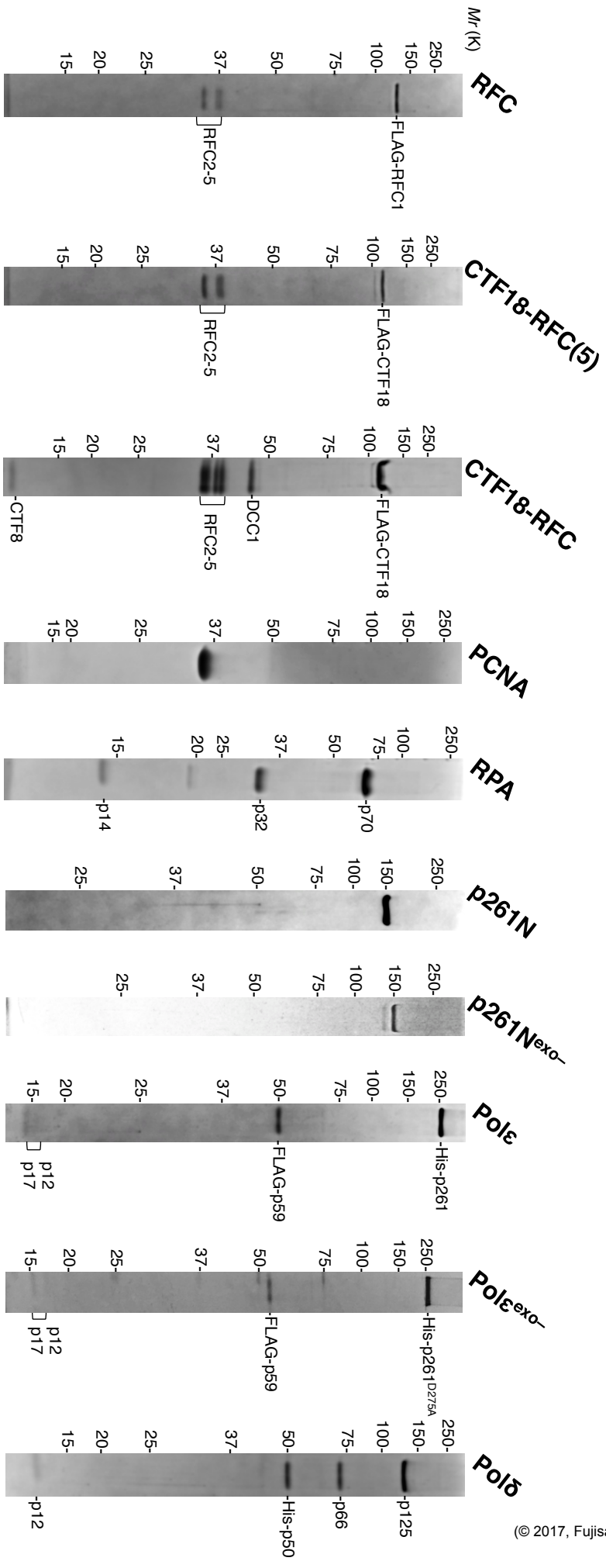

Figure 1

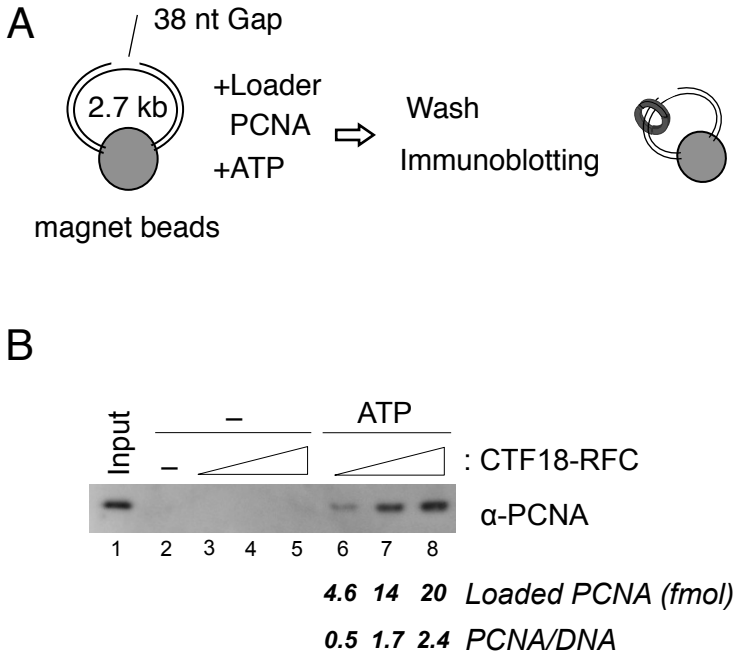

Figure 2

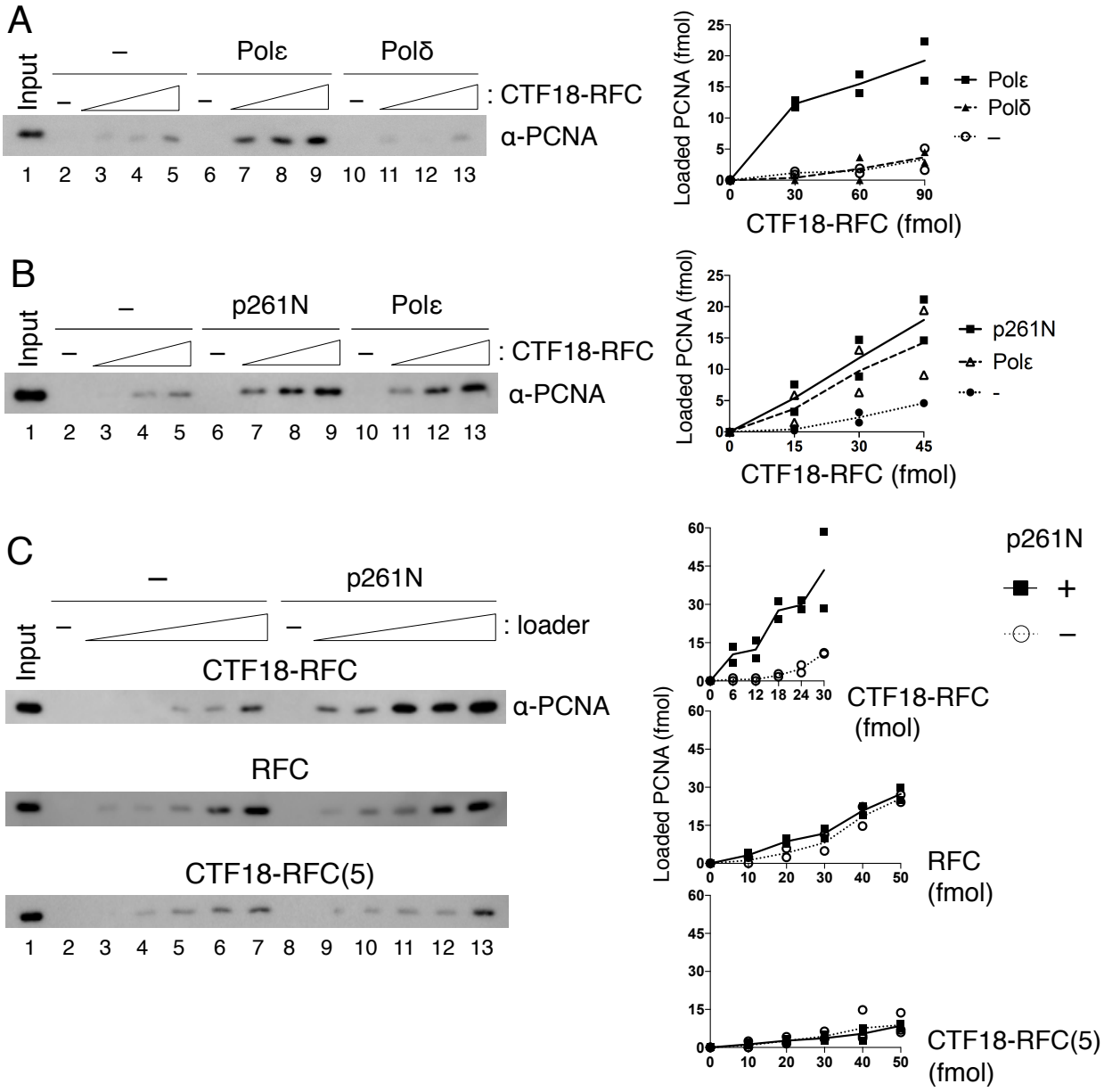

Figure 3

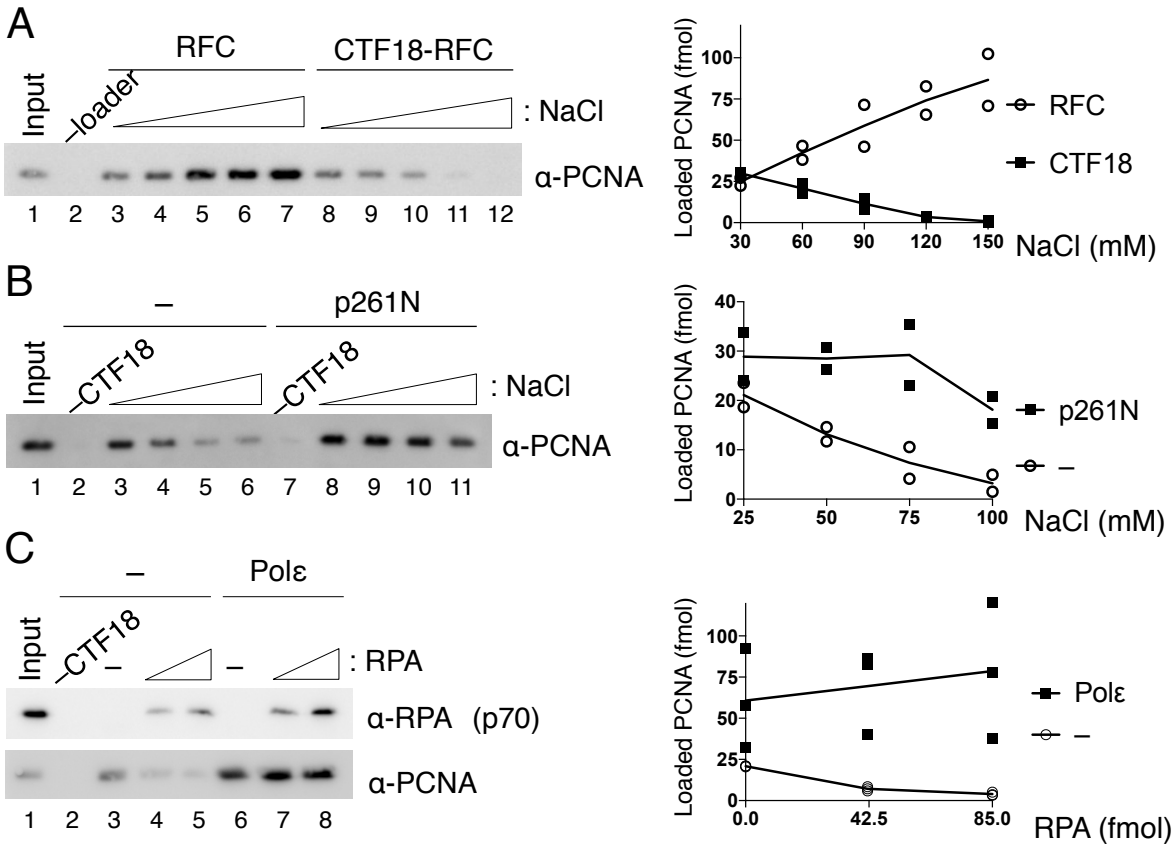

Figure 4

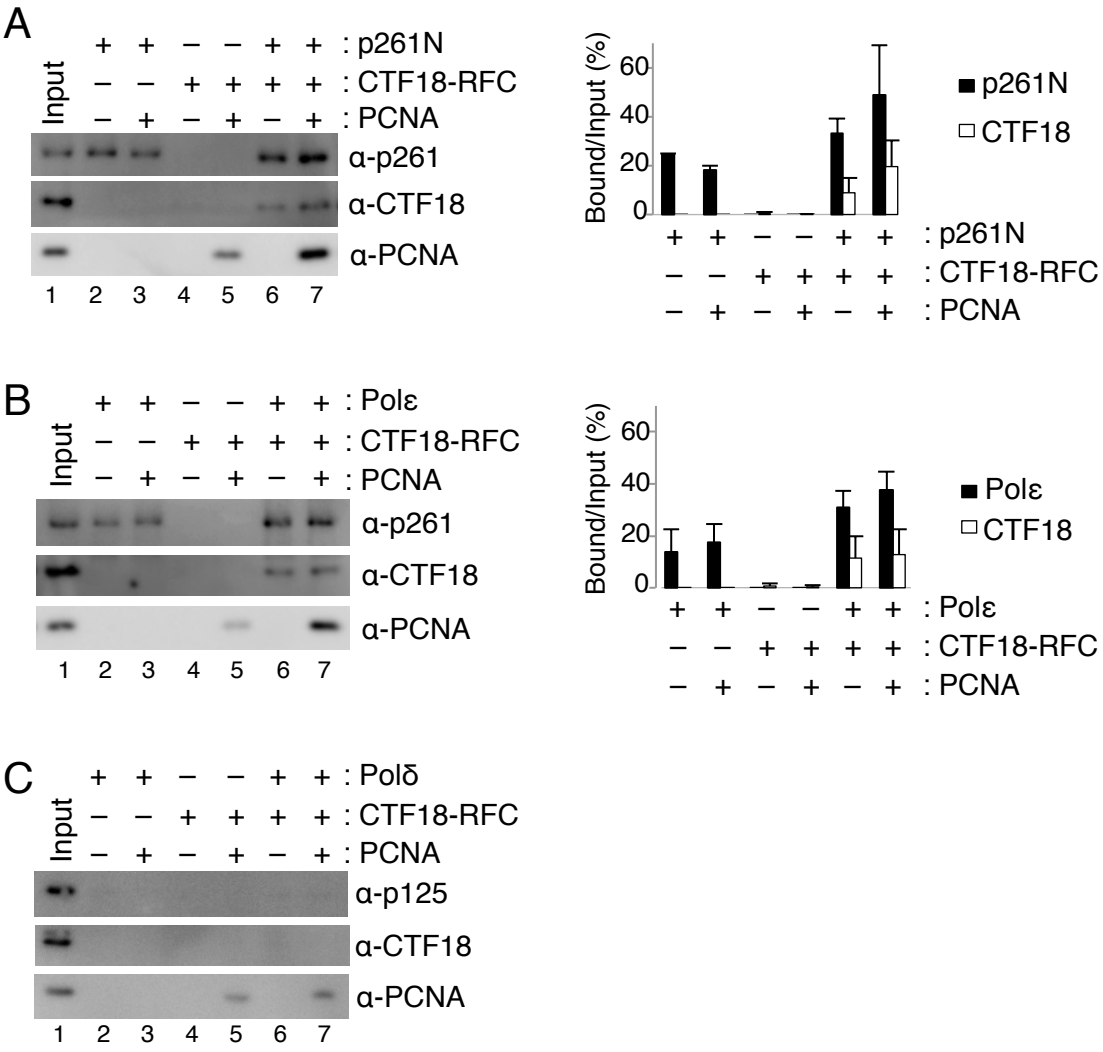

Figure 5

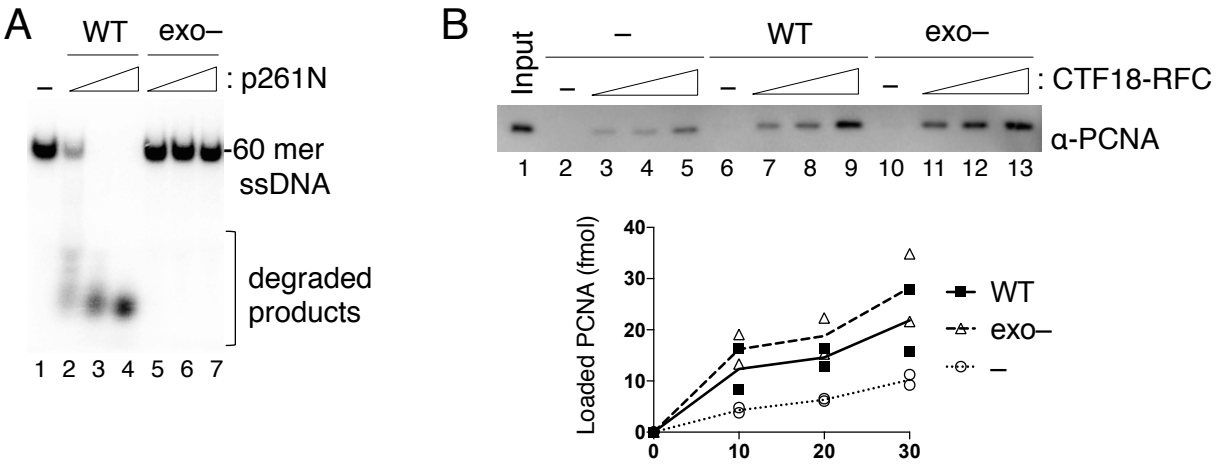

Figure 6

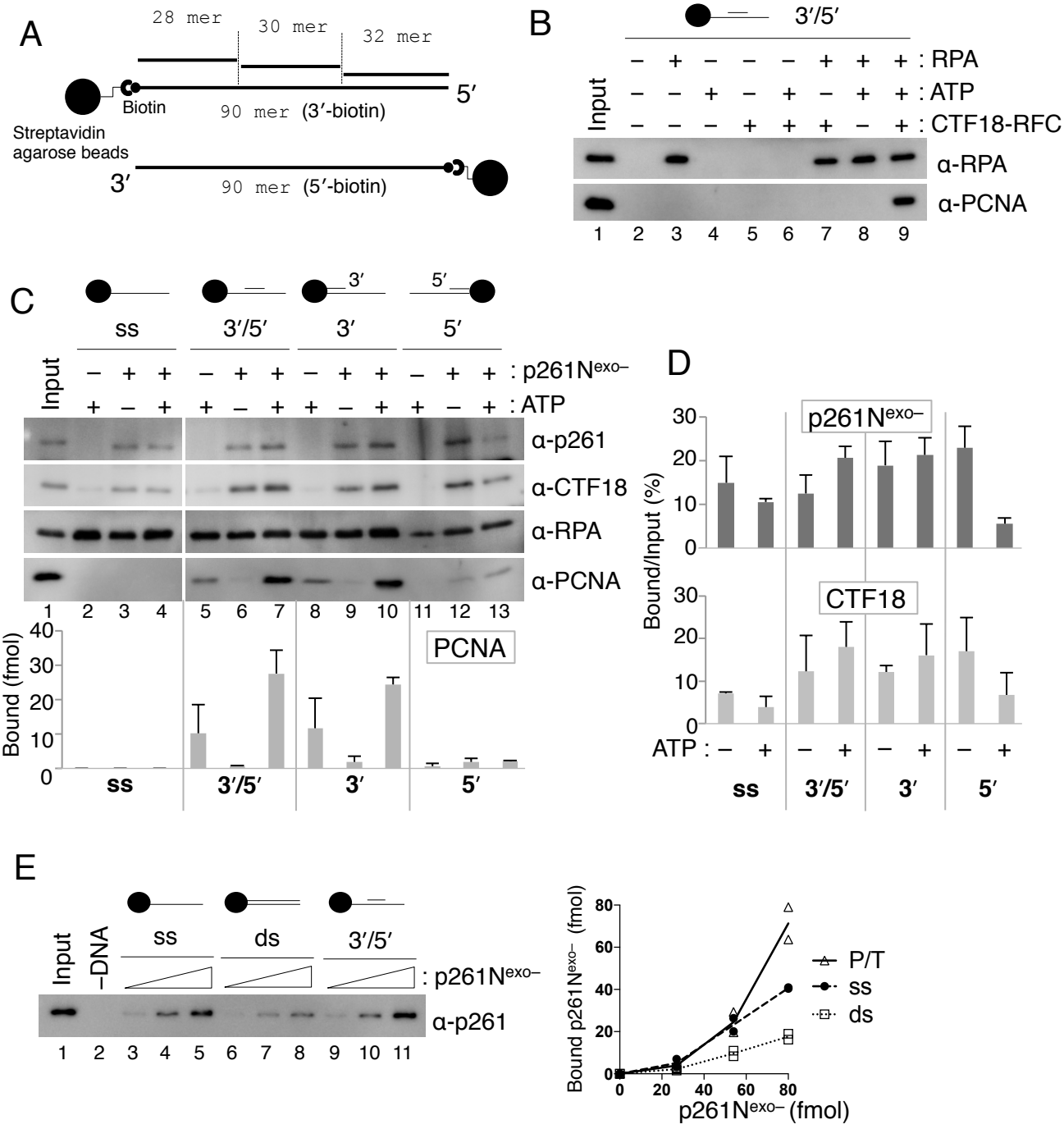

Figure 7

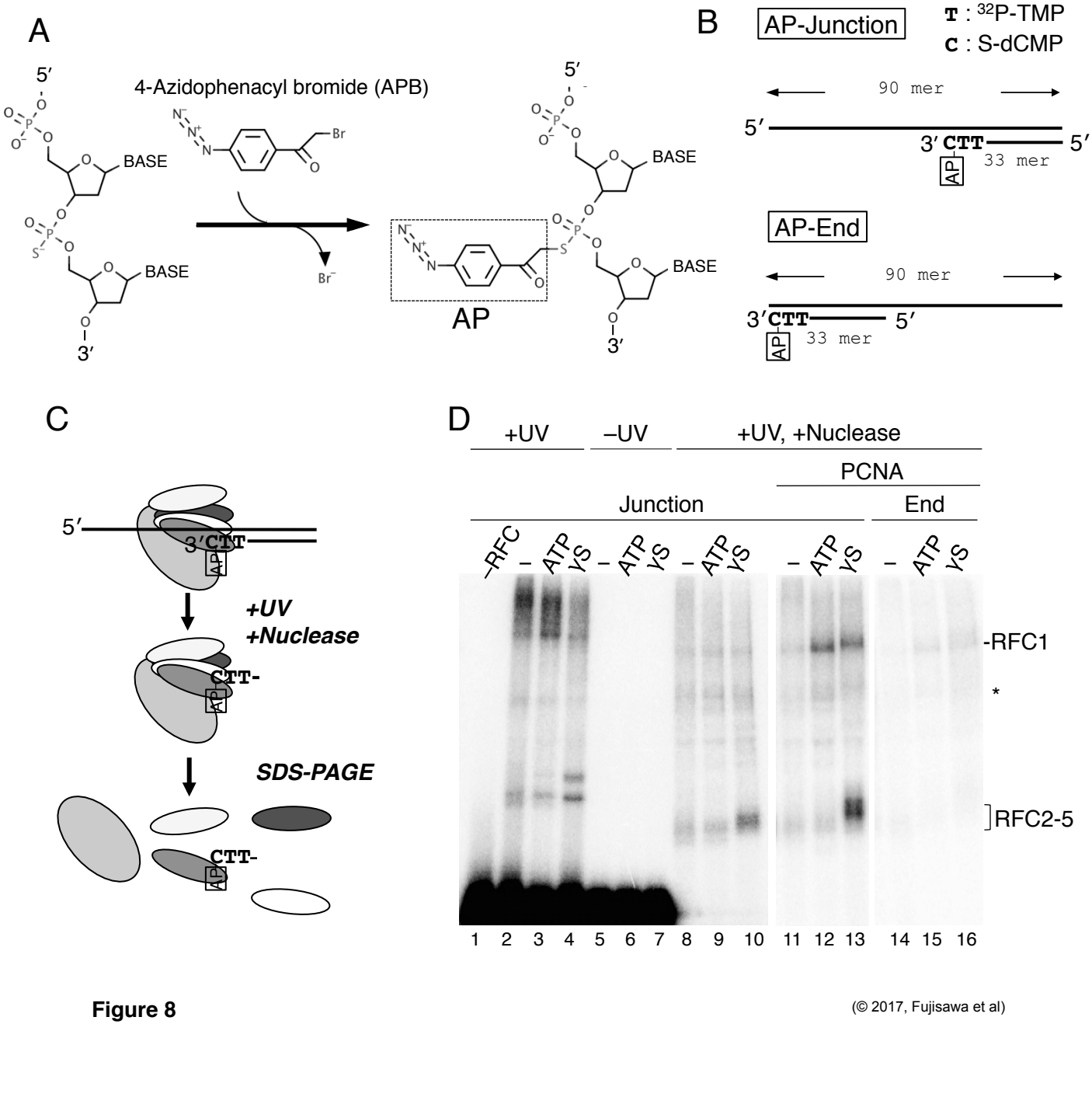

Figure 8

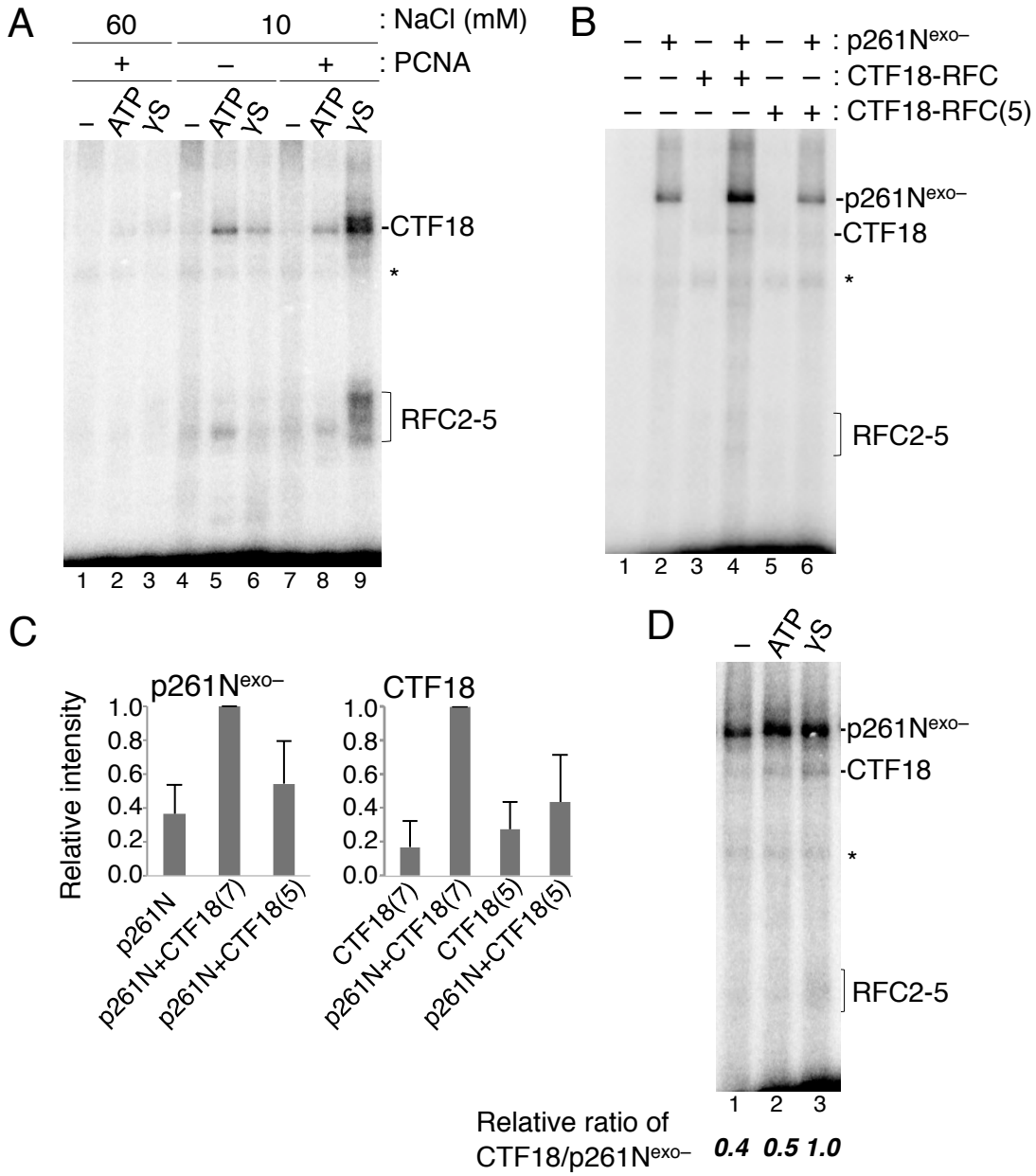

Figure 9

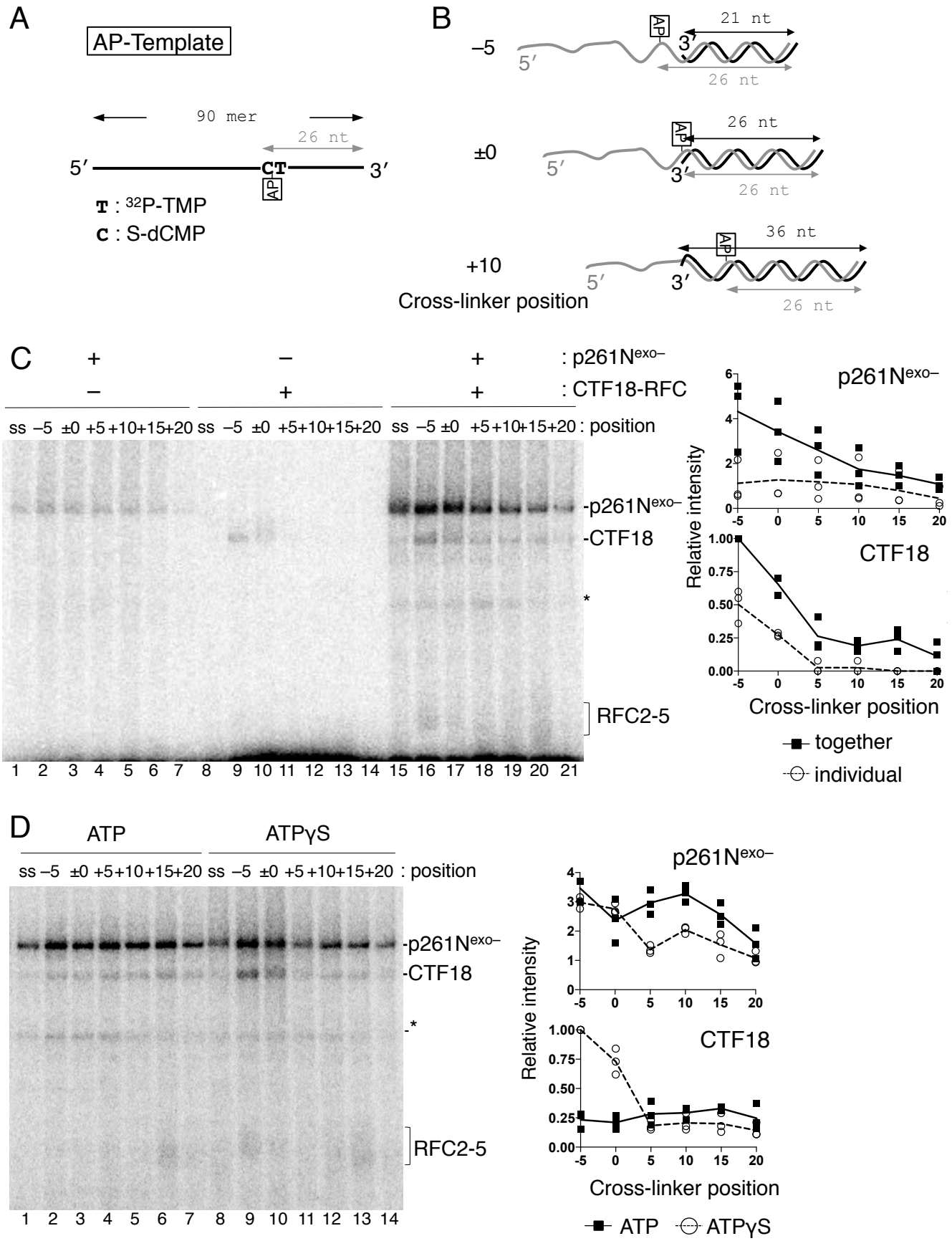

Figure 10

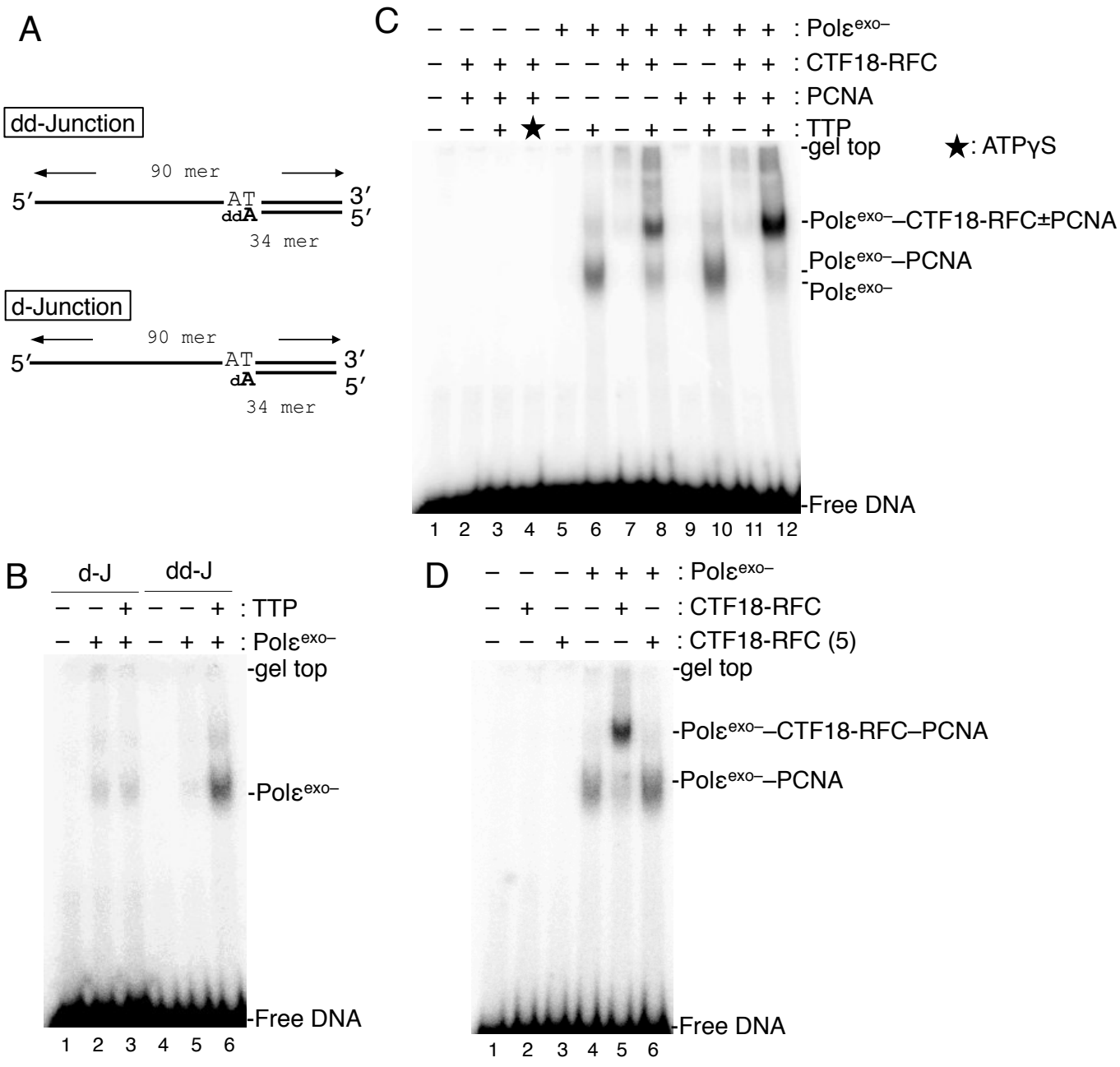

Figure 11

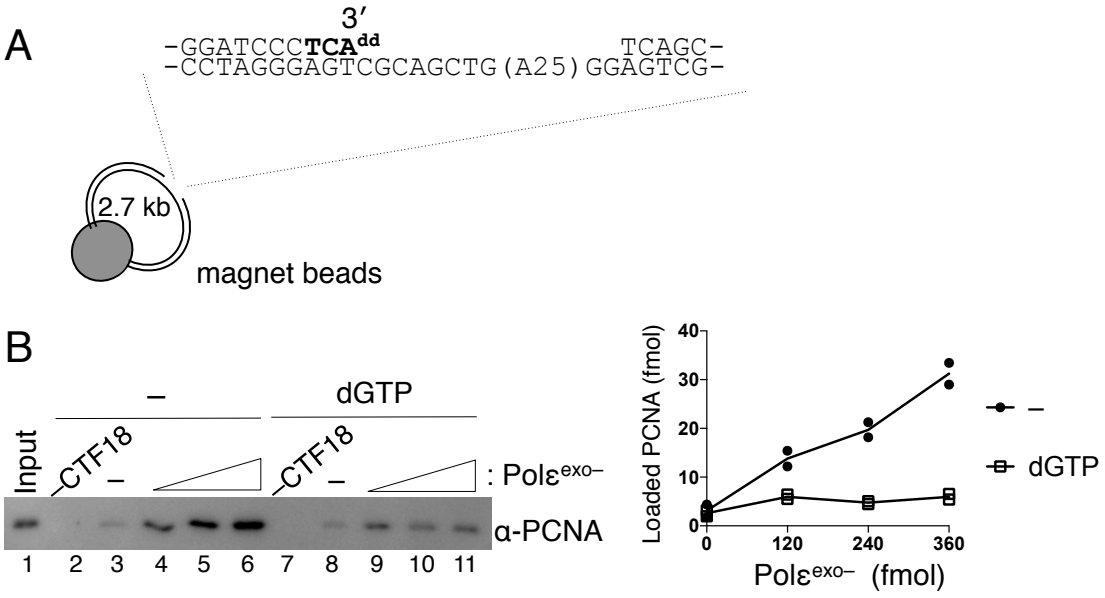

Figure 12

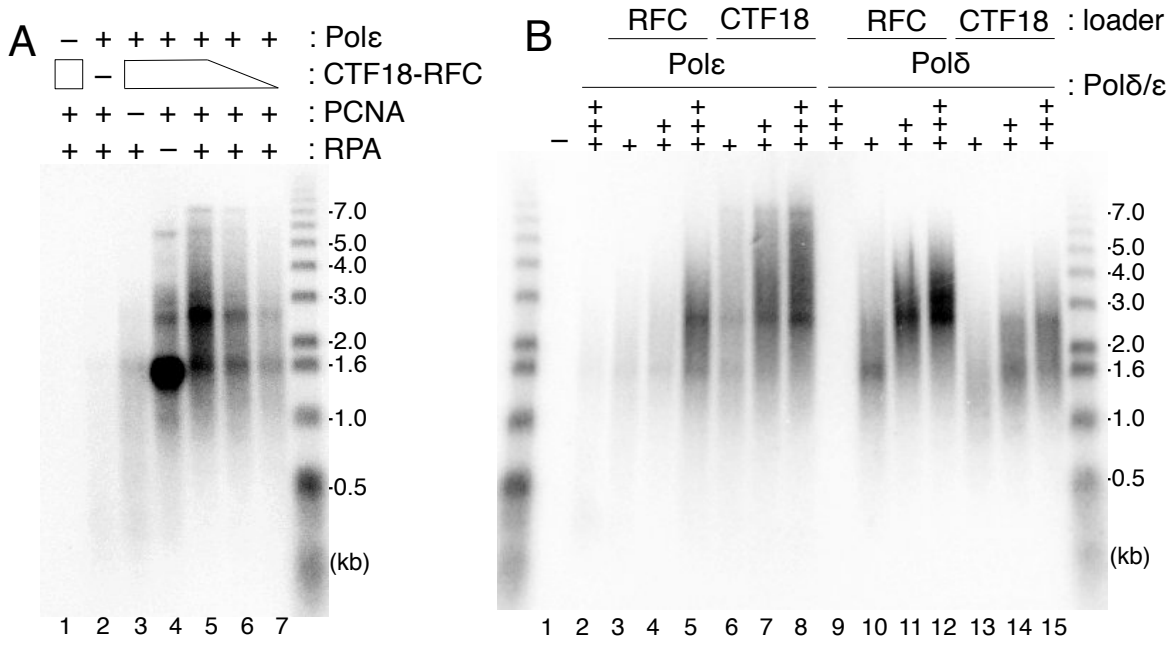

Figure 13

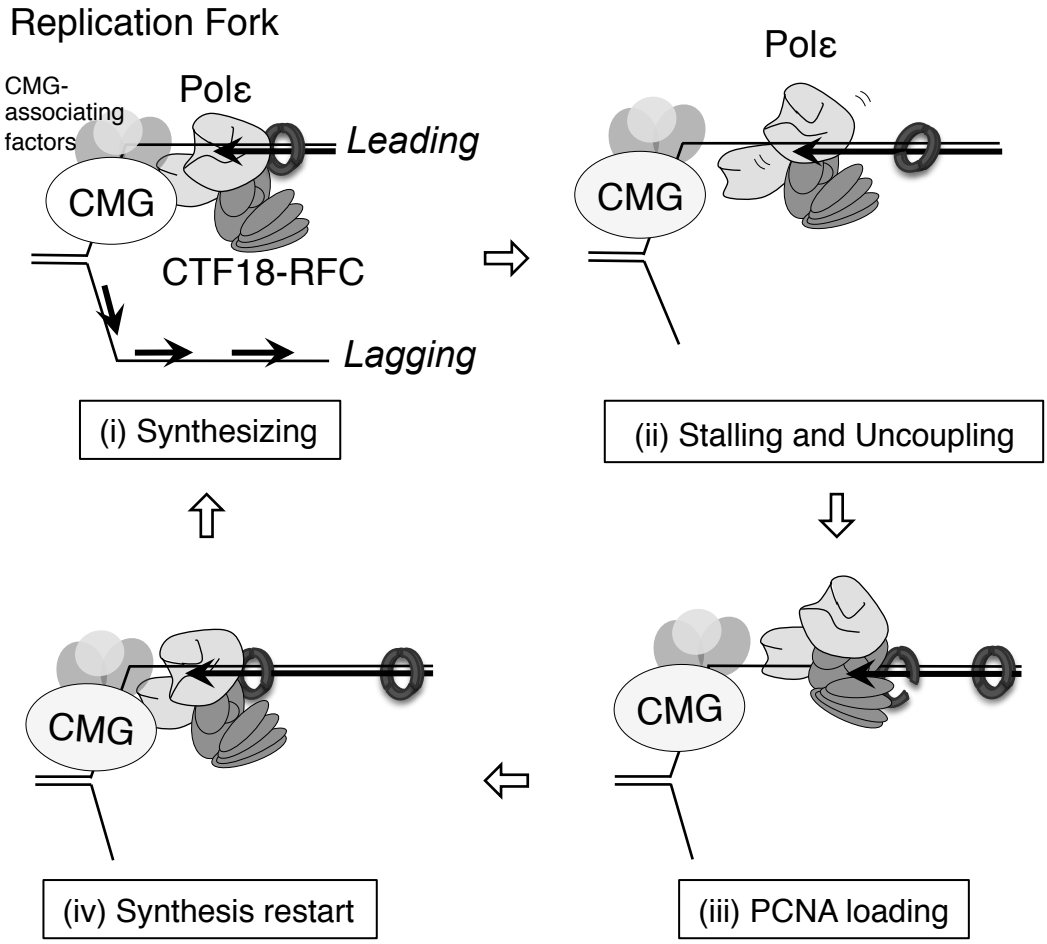

Figure 14